

2019-02

Early Ipswichian (last interglacial) sea level rise in the Channel region: Stone Point Site of Special Scientific Interest, Hampshire, England.

Briant, R

<http://hdl.handle.net/10026.1/11088>

Proceedings of the Geologists' Association

Elsevier

All content in PEARL is protected by copyright law. Author manuscripts are made available in accordance with publisher policies. Please cite only the published version using the details provided on the item record or document. In the absence of an open licence (e.g. Creative Commons), permissions for further reuse of content should be sought from the publisher or author.

Early Ipswichian (last interglacial) sea level rise in the Channel region: Stone Point Site of Special Scientific Interest, Hampshire, England

Rebecca M. Briant¹, Martin R. Bates², Steve Boreham³, Nigel G. Cameron⁴, G. Russell Coope⁵, Michael H. Field⁶, B., Marcus Hatch⁷, Jonathan A. Holmes⁴, David H. Keen⁵, Aiobhean A. Kilfeather⁷, Kirsty E.H. Penkman⁸, Rianne M.J. Simons⁶, Jean-Luc Schwenninger⁹, Francis F. Wenban-Smith¹⁰, Nicola J. Whitehouse¹¹, John E. Whittaker¹².

¹Department of Geography, Birkbeck, University of London, Malet Street, London, WC1E 7HX, UK.

²School of Archaeology, History and Anthropology, University of Wales Trinity Saint David, Lampeter Campus, Ceredigion, SA48 7ED, Wales.

³Department of Geography, University of Cambridge, Downing Place, Cambridge, CB2 3EN, UK.

⁴Environmental Change Research Centre, University College London, Pearson Building, Gower Street, London, WC1E 6BT, UK.

⁵Deceased.

⁶Faculty of Archaeology, Leiden University, P.O. Box 9515, 2300 RA Leiden, The Netherlands.

⁷School of Geography, Queen Mary, University of London, Mile End Road, London, E1 4NS, UK.

⁸BioArCh, Department of Chemistry, University of York, YO10 5DD, UK.

⁹Research Laboratory for Archaeology and the History of Art, Dyson Perrins Building, South Parks Road, Oxford, OX1 3QY, UK.

¹⁰Department of Archaeology, University of Southampton, Southampton, SO17 1BF, UK.

¹¹School of Geography, Earth and Environmental Science, University of Plymouth, Drake Circus, Plymouth, Devon PL4 8AA, UK.

¹²Department of Earth Sciences, Natural History Museum, Cromwell Road, London, SW7 5BD, UK.

Abstract

Constraining the speed of sea level rise at the start of an interglacial is important to understanding the size of the ‘window of opportunity’ available for hominin migration. This is particularly important during the last interglacial when there is no evidence for significant hominin occupation anywhere in Britain. There are very few finer grained fossiliferous sequences in the Channel region that can be used to constrain sea level rise and they are preserved only to the north of the Channel, in England. Of these, the sequence at Stone Point SSSI is by far the most complete. Data from this sequence has been previously reported, and discussed at a Quaternary Research Association Field Meeting, where a number of further questions were raised that necessitated further data generation. In this paper, we report new data from this sequence – thin section analysis, isotopic determinations on ostracod shells, new OSL ages and AAR analyses. These show early sea level rise in this sequence, starting during the pre-temperate vegetation zone IpI, but no early warming. The implications of this almost certainly last interglacial sequence for the human colonisation of Britain and our

understanding of the stratigraphic relationship of interglacial estuarine deposits with their related fluvial terrace sequences is explored.

Keywords AAR, OSL, interglacial sequence, sea level, estuary

1. Introduction

The last interglacial has been characterised as ‘deserted Britain’ (Ashton and Lewis, 2002), with no evidence of significant hominin occupation even after exhaustive review of multiple sequences (Lewis et al., 2011). Ashton and Lewis (2002) suggested that changes in hominin population density in Britain are controlled by two factors: the opening of the Dover Strait (and associated removal of a land bridge to the continent) and the rate of sea level rise at the start of an interglacial in relation to the rate of warming. Gupta et al. (2017) recently demonstrated that the opening of the Strait was a two-stage process, the second stage of which most likely occurred immediately prior to the last interglacial, although there is very little chronological control on this event. Once the land bridge had been removed, the rate of sea level rise becomes even more important, since hominins could not migrate once sea level had risen above the elevation of the sea floor (-40 m O.D. in the North Sea; -30 m O.D. at Dover; -60 m O.D. in the Channel). Therefore, to explain hominin absence from Britain during the last interglacial, when the Dover Strait had likely opened, constraining the rate of sea level rise is important to understand the size of the ‘window of opportunity’ available for hominin migration.

To constrain the rate of sea level rise at the start of the last interglacial, sedimentary sequences in the Channel region need to be investigated to complement the more northerly Dutch sequence (Long et al., 2015). However, shallow marine / coastal sequences in the Channel region are mostly clastic deposits that cannot be used to track sea level rise within the last interglacial (e.g. Bates et al., 2010, Pedoja et al., 2017). There are very few finer grained fossiliferous sequences that can be used to do this and they are preserved only to the north of the Channel, within the sheltered Solent seaway, peripheral to the main channel. (French sequences are more fragmentary and dated to earlier interglacials – e.g. Antoine et al., 2007). Of these, the sequence at Stone Point SSSI is the most complete (although of disputed age, which we discuss), and therefore the only sequence in the Channel region with the potential to constrain when sea level started to rise within the last interglacial, with associated impacts on hominin movement.

It is for this reason that this sequence was reinvestigated. Multiple fossil groups were analysed, from a much greater depth of sediments than previously recovered, with the aim of tracking sea level changes from the very start of the last interglacial. The Stone Point deposits comprise interbedded estuarine silts and peats exposed in the foreshore (Figure 1) and are associated with two gravel bodies (Figure 2). They have previously been assigned to both the last (Brown *et al.*, 1975) and the penultimate (Allen *et al.*, 1996) interglacial. Within the catchment of the former Solent river, interglacial deposits occur only at Stone Point (West and Sparks, 1960; Brown *et al.*, 1975); Pennington Marshes (Allen *et al.*, 1996); Bembridge Foreland (Preece et al., 1990) and St Leonards Farm (Briant *et al.*, 2013). These are all associated with the lower levels of the terrace sequence. At Pennington, St Leonard’s Farm and Bembridge Foreland, the deposits are of very limited depth (≤ 1.5 m), compared with the sequences at Stone Point (9.5 m). Early investigations at the site only cored the thinner, more onshore part of the deposits (2.5 m depth). The data presented in this paper spans the full 9.5 m of the sequence, studied as part of the ‘Palaeolithic Archaeology of the Sussex / Hampshire Coastal Corridor’ (PASHCC) project. Results have previously been partially reported by Briant *et al.* (2006a,b & 2009) and the site was visited by the Quaternary Research Association in April 2009. Following field discussion at the site further work was undertaken to: more firmly establish the age of the sequence (a maximum age constraint using AAR on shell from the base of Unit 2 and OSL on Unit 5); the nature of the contact between the interglacial deposits and the gravel in Unit 3 (thin section analysis); quantify the palaeotemperature during the deposition of Unit 2 using the mutual climatic range (MCR)

method and provide a salinity signal from Unit 2 (isotopic analyses). This paper presents these new results in the context of the full palaeoenvironmental results previously published. These key issues and wider implications are discussed below.

2. History of previous research

West and Sparks (1960) observed estuarine silty clays from *c.* –0.2 to –2.7 m O.D., including two beds with freshwater affinities, near boreholes 9, 11 and 12 (Figure 1). They stated that these lay stratigraphically between the upper and lower gravels. Pollen and macroscopic plant remains suggest deposition during a temperate period, dominated by *Quercus*, *Pinus* and *Acer*. Molluscan assemblages were dominated by the brackish species *Hydrobia*.

Brown *et al.* (1975) sampled the deposit to the north-east of the West and Sparks borehole, near test pits 6a and 6b (Figure 1) from *c.* +1.0 to –1.5 m O.D. They also observed but did not investigate organic deposits in a further channel in the foreshore *c.* 2.6 m to the east, beyond an expanse of lower gravel. The interglacial silts thinned onshore and were not observed within the cliffs, but a finer-grained deposit separating two gravel successions in the cliff was thought to be a continuation of a ‘pebbly clay’ observed beneath the silts. Pollen spectra were similar to those of West and Sparks (1960), with the addition of *Phragmites* and higher *Alnus*. In the plant macrofossil assemblages, freshwater species such as *Carex*, *Menyanthes trifoliata* and *Sparganium* were in the peat beds and saltmarsh species including *Glaux maritima* and *Scirpus maritimus* were present throughout. All mollusca recorded were brackish (*Hydrobia*) and they found a single vertebrate remain of *Dama dama* (fallow deer).

Overlying the upper gravel is a ‘brickearth’ deposit (Unit 5, Figure 2, Table 1), described by Brown *et al.* (1975) as 1 m thick. This was studied in greater detail by Reynolds (1985, 1987) who described a lower brickearth 40 cm thick overlain by an 80 cm thick upper brickearth in which a Holocene soil had developed. The lower brickearth was silty (90–93% silt) and the upper brickearth more sandy (33–45% sand). Reynolds (1985, 1987) ascribed the lower brickearth to an interglacial warm period because thin section analysis showed a period of clay illuviation, followed by disruption of clay argillans, suggesting frost activity following soil formation. It was suggested that the lower brickearth predated the last interglacial (Ipswichian), and the upper dated from the end of the last glacial period (Late Devensian). Parks (1990) later sampled a section at Stone Point and thermoluminescence (TL) dated the upper brickearth to the Late Devensian (*c.* 20 ka), and the lower brickearth to an earlier event at approximately 120 ka (Parks, 1990) or 98 ka (Parks and Rendell, 1992). This suggested that the palaeosol within the lower brickearth might have formed later, during interstadial conditions, although problems with zeroing the TL signal in sediments (see below) means that these ages are likely to be too old. Thus the age of these overlying silty sands (Unit 5) requires reinvestigation. The palaeosol is no longer exposed at the site, but Unit 5 is sufficiently thick to allow sampling for OSL dating.

West and Sparks (1960) and Brown *et al.* (1975) both attributed the Stone Point organic deposits to the Ipswichian (last interglacial, Marine Isotope Stage [MIS] 5e). Re-mapping of the Solent terrace deposits by Allen and Gibbard (1993) agreed with this age attribution. However, Keen (1995) reiterated the suggestion by Reynolds (1987) that it was likely the palaeosol separating the brickearth units is of Ipswichian (MIS 5e) age, implying the estuarine deposits must date to an earlier warm phase. This seemed to be reinforced by the identification of Ipswichian-age freshwater silts from –3.9 to –5.3 m O.D. at Pennington Marshes (Allen *et al.*, 1996; Gibbard and Preece, 1999; Bridgland, 2001; Antoine *et al.*, 2003), within the Pennington Gravel which was thought to postdate the Lepe Gravel. A further reinterpretation of the terrace stratigraphy led Bridgland (2001) to suggest an age of MIS 7a. Bridgland and Schreve, (2001), however, put forward the view that the (albeit sparse) mammal remains might point to a date in the earlier part of the MIS 7 interglacial. The relationship between the Pennington Gravel and the Lepe Gravel has since been queried by Westaway *et al.* (2006) who suggest that in places both fall within an alternative gravel body called the St Leonards Farm

Gravel. The stratigraphy of these lower terraces was not, however, fully defined in this scheme. Hatch (2013, et al., submitted), on the basis of detailed borehole analysis, confirmed that the Pennington Gravel was a separate deposit, and correlated the Lepe gravels with the Milford on Sea Gravel.

3. Materials and Methods

Sections through the deposits were exposed using a combination of mechanically-cleared sections (sections 1 and 5, 2003), mechanically-dug test pits (test pits 4-7, 2003), hand drilled boreholes (boreholes 8-13, 2004) and mechanically-recovered boreholes (boreholes 14-16, 2005). Samples were taken as bulk material, spot samples and as blocks of sediment for both fossil analysis and thin section investigation. Light-tight samples were also taken for OSL dating.

OSL dates from sections 1 and 5 and test pit 4a were published in Briant et al. (2006a); ostracods from test pits 4b, 4d, 7 and borehole 13 in Briant et al. (2006b) and full palaeoenvironmental data from all locations, including the newly drilled Borehole 16 in the QRA Field Guide (Briant et al., 2009). The age of the deposits (particularly Unit 5), nature of Unit 3 and salinity signal from Unit 2 were much debated at this meeting and so further analysis was undertaken to more firmly establish age (OSL from Unit 5, sampled in 2010, AAR from Unit 2), the nature of Unit 3 (thin section analyses) and salinity (isotopic analyses on ostracods).

Thin section analysis was undertaken on two samples from Unit 3 from Section 1 and Test pit 6a (Figure 2). Intact block samples were taken for thin section production. Thin sections were prepared using the methods outlined in van der Meer (1993). The thin sections were photographically recorded and features observed under a low power microscope.

Pollen samples were analysed from eight levels within Borehole 16 (previously reported in Briant et al., 2009) and an additional sample from Unit 3 in March 2016, which proved to be barren. These were prepared using the standard hydrofluoric acid technique and counted for pollen using a high-power stereo microscope. Pollen preservation was relatively good, although some samples showed evidence of post-depositional oxidation. Main sums varied between 105 and 291, and pollen concentrations varied widely between 23412 and 258966 grains per ml. It should be noted that for statistically reliable data, pollen sums of at least 300 are generally recommended. These counts rarely reach these levels, and care must therefore be taken during interpretation.

Plant macrofossils were analysed from four samples from BH16 Table 2). They ranged in size from 100ml (740-746 and 750-755cm) to only 50 ml (761-768 and 772-777 cm). The sediment samples were soaked in water and then wet sieved through a nest of sieves (down to a 150 µm mesh size). Macroscopic plant remains were then picked from the resulting residues.

Molluscan analysis was undertaken on 7 samples from test pits 4d and 6a by Professor David H. Keen (Table 3). Samples from Borehole 16 (drilled in September 2005) were not completed because of his death, although a brief scan of the samples was undertaken by Dr R.C. Preece, as discussed below. The samples were washed through sieves to 500µm aperture, dried and sorted under a 10-60x binocular microscope. Counting conventions follow Sparks (1961) in which each gastropod apex is recorded as a single individual, and each bivalve hinge line as half an individual. Taxonomic nomenclature follows the usage of Seaward (1990).

Coleopteran analysis was undertaken on 13 samples from test pits 4b, 4d, 6a, 6b and 7, borehole 16 and a small test sample collected in 1974 from the organic deposit exposed on the foreshore about three metres to the west of the southern end of the measured section AA of Figure 3 of Brown et al. (1975) (Table 4). Most of the samples come from Unit 2d, but one sample from the base of Borehole 16 fell within Unit 2b. The more organic horizons were intensely compressed and difficult to break down. Samples were therefore frozen for several hours, followed by washing in hot water and gentle manual splitting of the layers along the

bedding planes. The resultant slurry was then washed over a 0.25 mm mesh and the insects concentrated by paraffin flotation (Coope 1986). In many cases the insect fossils were flattened and appeared rather decomposed and pale. The nomenclature and taxonomic order follow that of Lucht (1987). The numbers opposite each species and in each sample column indicate the minimum numbers of the species in the sample. Non-British species are indicated by *

Quantification of the climate signal from the coleopteran assemblages was undertaken using the Mutual Climatic Range (MCR) method (Atkinson et al. 1987). This was automated using the BugsMCR function of the BugsCEP database (Buckland & Buckland 2012). TMax (mean July air temperature) and TMin (mean January air temperature) were calculated for Units 2b and 2d separately. These temperature estimates are based on the thermal climate requirements of carnivorous and scavenging beetle species with food requirements that are independent of particular macrophytes or terrestrial plants.

Ostracod and foraminiferal analysis was carried out on 44 samples from test pits 4b, 4d and 7 and boreholes 13 and 16 (Table 5). The samples were first placed in ceramic bowls and dried thoroughly in an oven. Each was then covered in boiling water (with a little sodium carbonate added to help release the clay fraction) and allowed to soak. They were washed through a 75 micron sieve with hot water. The remaining residue was then decanted back into the bowl which was placed in the oven again, to dry. When dry, the samples were stored in plastic bags. Each sample was then dry-sieved into various fractions and the residue little-by-little sprinkled onto a metal picking tray, a representative number of each species being picked out under a binocular microscope and placed in a 3x1" faunal slide. A semi-quantitative estimate of the abundance of each species was also noted. It was not possible to quantify palaeotemperatures from the ostracod assemblages because they contained exclusively brackish water species, and the Mutual Ostracod Temperature Range (MOTR) method is currently applicable only to non-marine/freshwater assemblages (Horne, 2007).

Diatom analysis was undertaken on 7 samples from borehole 16. Preparation followed standard techniques: the oxidation of organic sediment, removal of carbonate and clay, concentration of diatom valves and washing with distilled water (Battarbee 1988). Two coverslips, each of a different concentration of the cleaned solution, were prepared from each sample and fixed in a diatom mounting medium (Naphrax) of a suitable refractive index for microscopy. Slides were scanned and counted at magnifications of x400 and x1000 under phase contrast illumination. Diatom species' salinity preferences are discussed using the halobian groups of Hustedt (1953, 1957: 199), these salinity groups are summarised as follows:

1. Polyhalobian: >30 g l⁻¹
2. Mesohalobian: 0.2-30 g l⁻¹
3. Oligohalobian - Halophilous: optimum in slightly brackish water
4. Oligohalobian - Indifferent: optimum in freshwater but tolerant of slightly brackish water
5. Halophobous: exclusively freshwater
6. Unknown: taxa of unknown salinity preference.

Trace-element (Mg/Ca and Sr/Ca) and stable-isotope (¹⁸O/¹⁶O and ¹³C/¹²C) determinations were undertaken on shells of the ostracod *Cyprideis torosa* from 11 samples from test pits 4b, 4d and 7 and borehole 13 (Table 6). Unfortunately, by the time isotopic analyses were undertaken on these samples, samples from borehole 16 were no longer available. Well-preserved shells of *C. torosa* lacking signs of calcite overgrowth or dissolution were chosen, brush-cleaned and air dried in preparation for trace-element and stable-isotope

analyses. All shells selected for analysis were smooth morphotypes and adults. Five single shells from each chosen level were placed in separate acid-washed 5 mL polyethylene tubes, dissolved in 2 mL of Aristar grade HCl acid and analysed for Ca, Mg and Sr using a JY Ultima 2C ICP-AES calibrated using BDH Spectrosol mono-element standards for ICP. Results were corrected for blank contamination and for instrumental drift using an external drift monitor and expressed as molar trace-metal to Ca ratios for plotting purposes. Instrumental precision was ± 1.2 % and ± 2.4 % RSD for Mg/Ca and Sr/Ca, respectively. Multiple-shell (4 adult shells per sample) samples were analysed for oxygen and carbon isotopes using a ThermoFinnigan Delta Plus XP mass spectrometer connected to a GasBench. Results were expressed in delta units relative to the VPDB standard. Typical precision was ± 0.05 ‰ for both $\delta^{18}\text{O}$ and $\delta^{13}\text{C}$. Methods used to estimate temperature and salinity from these results are discussed in the results section below.

Four OSL samples from Unit 5 were prepared to quartz in the same way as those reported in Briant et al. (2006a). This involved separation of the modal size fraction by wet sieving and treatment with hydrochloric and hydrofluoric acids and removal of heavy minerals using sodium polytungstate. Samples with feldspar contamination (detected using infra-red (IR) light stimulation, Hütt et al., 1988) were subjected to further treatment in fluorosilicic acid. Palaeodose was determined in the Research Laboratory for Archaeology and the History of Art, Oxford, using automated Risø measurement systems with both blue diodes and green halogen light (Briant et al., 2006a). The Single Aliquot Regenerative (SAR) protocol of Murray and Wintle (2000) was used, with the addition of a post-IR blue OSL procedure (Banerjee et al., 2001) to further minimise feldspar contributions. Single aliquot luminescence measurements were made at 125°C, with preheat 1 (PH1) of 260°C for 10 s, preheat 2 (PH2) of 220°C (initial measurements) or 240°C (additional measurements) for 10 s and up to 6 regeneration dose points. Initial measurements on all four samples were on aliquots 6 mm in diameter and comprised grains in the 180 to 255 μm fraction, meaning that c. 700-850 grains were present on a disc, of which c. 35-45 are likely to be active (Duller, 2008). Additional measurements on X4103 and 4105 were on aliquots 3-4 mm in diameter and also the 180 to 255 μm fraction, giving c. 150-500 grains on a disc, of which c. 7-25 are likely to be active (Duller, 2008). Equivalent dose (De) is a weighted mean of between 10 and 24 aliquots. Luminescence behaviour was very good, with low IRSI values suggesting minimal presence of feldspars and good recycling (Table 7).

Environmental dose rates for the Unit 5 ages were calculated on the basis of Inductively-Coupled Plasma Mass Spectrometry (ICP-MS). Radioisotope concentrations were converted to dose rates using the conversion factors of Adamiec and Aitken (1998) and grain-size attenuation factors of Mejdahl (1979). Cosmic dose rates were calculated using the equation of Prescott and Hutton (1994) and it was assumed that overburden accumulated soon after deposition and was negligible relative to the burial period. Interstitial water content attenuates dose rates, and this was corrected for using the absorption coefficient of Zimmerman (1971). It was assumed that present-day moisture content was representative of water contents throughout burial (percentage dry weight of sample) with a 5% error to reflect uncertainty in estimation. Ages were calculated by dividing the mean equivalent dose (De) by dose rate and presented as \pm one standard error (i.e. standard deviation / \sqrt{n}).

AAR analyses were undertaken on two small individual *Bithynia tentaculata* opercula from Unit 2c within BH16 between 754 and 756 cm depth (NEaar 3312-3313). Samples were prepared using the procedures of Penkman et al. (2008) to isolate the intra-crystalline protein by bleaching. Two subsamples were then taken from each opercula; one fraction was directly demineralised and the free amino acids analysed (referred to as the 'Free' amino acids, FAA, F), and the second was treated to release the peptide-bound amino acids, thus yielding the 'total' amino acid concentration, referred to as the 'Total hydrolysable amino acid fraction' (THAA, H*). Samples were analysed in duplicate by RP-HPLC.

The revised technique of amino acid analysis developed for geochronological purposes (Penkman et al., 2008) combines a recent reverse-phase high-pressure liquid chromatography (RP-HPLC) method of analysis (Kaufman and Manley, 1998) with the isolation of an 'intra-crystalline' fraction of amino acids by bleach

treatment (Sykes et al., 1995). This combination of techniques results in the analysis of D/L values of multiple amino acids from the chemically protected (closed system) protein within the biomineral, thereby enabling both decreased sample sizes and increased reliability of the analysis. Amino acid data obtained from the intra-crystalline fraction of the calcitic *Bithynia opercula* indicate that this biomineral is a particularly robust repository for the original protein (Penkman et al., 2011) and therefore has been targeted in this study.

4. Results

4.1 Description of sedimentary sequence

The lowest member of the Quaternary succession at Stone Point is an angular flint gravel (Unit 1 – Lepe Lower Gravel) whose lower contact was not observed in detail, representing a gravel aggradation of the former Solent River. It is a 2.5 m thick planar-cross-bedded gravel with thick sand bed, present both beneath the modern beach and in the lower part of the cliff succession up to a level of c. 3 m O.D. (Figure 2, Briant et al., 2009). West & Sparks (1960) suggested that the lower gravels and estuarine deposits pass beneath the upper gravels exposed in the cliff. Following a period of cliff erosion Brown *et al.* (1975) traced only the lower gravels into the cliff up to a level of about 2 m O.D., a metre lower than observed in 2003 (Briant et al. 2009). Brown et al. (1975) suggested that this lower gravel was succeeded by a thin bed of inorganic pebbly clay about 25cm thick; also in some places a bleached sandy horizon and iron pan suggesting podsolisation of the upper part of the lower gravel. PASHCC excavations did not find this ‘pebbly clay’. Instead, a thin sand and silt bed (Unit 3) was observed both overlying the interglacial silts in Test pit 6b and between the two gravels (Units 1 and 4) in section 1 (Figure 2). Unit 3 was noticeably thicker (c. 10-15 cm) in exposures to the east of PASHCC section 5 observed by BB in March 2016. A sample from this thicker exposure was prepared for pollen analysis but proved to be barren.

The full extent of Units 1 and 2 is unknown, but they are not present at Lepe Coastguard House, 0.6 km west of Stone Point (Reynolds, 1987), or at Cadland, 2 km to the north. At both these locations a low terrace gravel of the River Solent rests directly on Tertiary bedrock, its base at approximately the same level as the base of the upper gravel (Unit 4) at Stone Point. The estuarine deposits and lower gravel at Stone Point appear, therefore, to occupy a depression cut in Tertiary bedrock to altitudes below present sea level.

Unit 2 comprises the Stone Point interglacial deposits. Units 2a to 2c are only recorded from the deeper interglacial sequence recovered by the PASHCC project from Borehole 16 (Figure 2). These yielded some fossils with freshwater affinities (Table 2). Unit 2a is a cemented fine sand and silt with frequent gravel including chalk, conformably overlain by Unit 2b which is characterised by dark brown, fine sandy organic clay and fibrous peat. This in turn is conformably overlain by Unit 2c which comprises an interbedded laminated brown organic clay and grey clay with lenses of fibrous peat and fine sand containing molluscs.

However, the bulk of the sequence is represented by Unit 2d - a stiff grey clay with shells, interbedded with thin discontinuous beds of compressed wood-peat, especially in the upper parts of the profile. These peat beds were labelled A to E by Brown *et al.* (1975) and noted to be between 2 and 24 cm thick and containing abundant *Phragmites* remains. These higher estuarine peats and clays are separated into two outcrops occupying depressions in the lower gravel separated by a gravel high. The uppermost clays show signs of weathering and attain an altitude of about 0.8 m O.D. The peat layers are highly compressed. West and Sparks (1960) described organic sediments from a site lower down on the foreshore, probably from a level lower in the succession than those described by Brown *et al.* (1975). The estuarine deposits of Unit 2d have yielded coccoliths, pollen, abundant plant macrofossils, molluscan remains, the partial tusk of a straight-tusked elephant (*Palaeoloxodon antiquus*) and a tibia of a fallow deer *Dama dama* (West and Sparks 1960; Brown *et al.*, 1975; Preece *et al.*, 1990; Briant et al., 2006b, 2009).

Unit 3 is a discontinuous 5–10 cm thick bed of laminated fine sand and silt, overlying a sharp contact at the top of Units 1 and 2 depending on location (Figure 2). Two samples were taken from this unit by PASHCC for thin section analysis (Figures 2 and 3). Structures observable in the field are fine laminae, distorted in places in Section 1. Thin section analysis also showed that this unit comprised interbedded sands and silts/clays, with some distortion of clays in Section 1 (Figure 3a). Neither thin section showed widespread evidence of soil formation, e.g. translocated clays or void filling. In Section 1 there was a single cross-section of an organic item (root or stem), surrounded by a void in which some clay had built up (Figure 3b). This is probably a modern intrusion into the section because gorse scrub was cleared from the section. The similarity between the samples from the two sections (Figures 3a, 3c) suggests that this unit is an effective stratigraphic marker placing the interglacial deposits between the two gravels. It is interpreted as a period of low-energy, fine-grained deposition, later distorted either by loading of saturated sediments or periglacial activity. A sample was prepared for pollen analysis in March 2016 but proved to be barren.

The Lepe Upper Gravel (Unit 4) is 3 to 3.5 m of horizontally-bedded flint-dominated gravels with occasional thin sand lenses, erosionally overlying Unit 3. It is interpreted as a fluvially-deposited gravel of the former Solent river, partly due to the lithological composition (Allen and Gibbard, 1993). Cross bedding observed in some of the finer sandy material, indicated an easterly flow direction from approximately 280°N (Brown *et al.*, 1975). There is some evidence for periglacial modification of the upper gravel since involutions and stone erections are weakly developed in its upper levels. The surface of the gravel at Stone Point was considered by Brown *et al.* (1975) to equate with the terrace surface that is widespread at about 7-8m O.D. between Calshot and Lymington and mapped as Lepe Gravel by both Allen and Gibbard (1993) and Westaway *et al.* (2006).

Unit 5 comprises 50 cm to 1 m of silty fine sand with dispersed fine pebbles gradationally overlying Unit 4. At present, this is exposed sporadically at the top of the sequence (Briant *et al.*, 2009, Figure 2), showing some modern soil development in places (Section 1) and bricks and roots in others (Section 5). Table 1 compares this deposit in 2010 with descriptions by Reynolds (1985) and Parks (1990), both of whom described the cliffs before the brickearth was disturbed by construction on top of the cliff (Reynolds, 1985). They described a two part deposit, with a discontinuous lower brickearth up to 40 cm thick separated from an upper brickearth up to 80 cm thick by a line of flints. Both these deposits showed evidence of soil development with the palaeosol separating the two units perhaps representing an interglacial soil (Reynolds, 1987). There is currently no evidence for palaeosol development within Unit 5, suggesting that the sequence that is currently exposed is likely to be truncated compared to what was exposed in the 1980's.

4.2 Palaeoenvironmental analyses

4.2.1 Pollen analysis

Pollen analysis reported here (Figure 4) is from borehole 16 only, to capture the base of the sequence. Combination of this with the upper part of the sequence reported by West and Sparks (1960, Figure 12) enables the full vegetation succession to be discussed. Starting from the base of the sequence, the basal samples (7.46 m [base of Unit 2d], 7.57 m [Unit 2c] & 7.73 m [Unit 2b]) were dominated by grass (c.31.3–35.1%) and pine (c.13.2–18.3%) with sedges (Cyperaceae) (c.4.8–11.3%) and spruce (*Picea*) (1.8–3.5%). These samples also had elevated proportions of *Pteropsid* spores (c.9.5–18.4%) and pollen of the aquatic bur-reed (*Sparganium*) (c.7.3–24.9%). The sample from 7.46 m is interesting in that it represents something of a transition, with the first occurrence of oak, and an increase in the frequency of hazel, juniper (*Juniperus*) and birch (*Betula*). These lower samples record a boreal grass-pine phase and can be assigned to the pre-temperate stage (I) of the interglacial.

Above this, in Unit 2d, there is a significant difference between those samples analysed from the lower part of the unit in borehole 16 and those analysed from the upper part of the unit by West and Sparks (1960). Those samples from borehole 16 had a relatively homogeneous assemblage dominated by grass (Poaceae), hazel (*Corylus*), oak (*Quercus*) and pine (*Pinus*). Subtle changes in the proportion of herbs such as buttercup

(*Ranunculus*) and strapwort plantain (*Plantago lanceolata*) can be seen, and the minor arboreal taxa present included elm (*Ulmus*), alder (*Alnus*), ash (*Fraxinus*), maple (*Acer*), willow (*Salix*) and holly (*Ilex*). This part of the sequence represents a temperate mixed-oak woodland environment that can be assigned to the early temperate stage (II) of the interglacial. The lower percentages of *Quercus* and *Corylus* compared to the West and Sparks (1960) sequence suggest assignment to substage IIa, since they assigned their sequence to substage IIb (Phillips, 1974). There may be some indication of estuarine sedimentation in that pollen of the fat hen family (Chenopodiaceae) appears to increase towards the top of the sequence. Emergent aquatic vegetation (bur-reed) appears to be present throughout.

In the upper part of the sequence reported by West and Sparks (1960) and Brown et al. (1975), pollen analysis suggests the presence locally of mixed-oak woodland. These authors assigned the sequences that they observed to zone IIb of the Ipswichian with the presence of *Carpinus* indicating a position late in this zone. Herbaceous pollen mainly comprises Poaceae and Chenopodiaceae which reaches 54% AP in some peat beds, perhaps suggesting saltmarsh conditions during deposition of this upper organic layer (Brown et al., 1975). There is a gradual increase in hazel (*Corylus*) pollen upwards.

4.2.2 Plant macrofossils (Michael H. Field & Rianne M. J. Simons)

The limited diversity and small size of the samples mean that it is difficult to identify any significant changes in the composition of the assemblages and the four samples from borehole 16 are therefore discussed together (Table 2). Waterside and damp ground taxa are dominant in all the assemblages, suggesting significant swamp vegetation at the margin of the water-body. Particularly common is *Typha* sp., but also present were *Eleocharis* cf. *palustris*, *Sparganium erectum*, *Juncus* sp. and *Carex* sp. Further away from the water-body, there is evidence of only two tree taxa. *Betula* probably grew in the drier areas surrounding the site, while *Alnus glutinosa* was present where conditions were damp.

In contrast, aquatic taxa are not well represented in the assemblages, but do give some indication of salinity. The floating aquatic *Hydrocharis morsus-ranae* requires still, fresh-water conditions and is present in the two lower samples from Units 2b and 2c. However, the samples from Unit 2d yielded one fruit of *Ruppia* and *Scirpus maritimus* which both suggest a degree of salinity at the time of deposition. *Zannichellia palustris* also occurs in Unit 2d. This is a species that lives in fresh-water but can also tolerate a degree of salinity. It is unlikely that the fresh-water and brackish components of the assemblages inhabited the site at the same time, and indeed there is some evidence that the freshwater elements are concentrated in the lower parts of the sequence and the more saline elements in the higher parts. Where there is mixing, taphonomic processes may have washed the fresh-water component down into the tidal zone or a fresh water-body was occasionally inundated by saline water bringing with it the remains of salt tolerant plants.

4.2.3. Molluscs (David H. Keen)

Molluscs are only described from Unit 2d (Test pits 4 and 6, Table 3), because of the untimely death of David Keen before analysis of borehole 16. The fauna from Unit 2d described here differs little to that reported from previous publications (West & Sparks, 1960; Brown et al., 1975). Preservation of shell was patchy and the fauna composed overwhelmingly of Hydrobiidae with fragments of *Scrobicularia plana*. The current study notes the occurrence of two further bivalve taxa, *Cerastoderma edule* and *Abra* spp, taking the total fauna to 6 species. This fauna suggests brackish conditions in a lagoon or estuary. It is not certain whether the site of deposition was a lagoon or the mud banks of an estuary. The preference of *H. ventrosa* for sites sheltered from direct contact with estuarine waters and tides (Kerney, 1999) perhaps indicates a lagoon for the site of deposition. This possibility is reinforced by the total lack of any freshwater shells in Unit 2d. In the present and the two previous studies *H. ventrosa* is more numerous than *H. ulvae* at most levels, although West & Sparks (1960) record a majority of *H. ulvae* near the bottom of their borehole at depths below 92 cm. The mean salinity values from comparing the ranges of these species (after Peacock, 1993) are 20-25‰ (current

salinity tolerances of *H. ventrosa* are between 6 and 25 ‰; *H. ulvae* between 10 and 40 ‰; *S. plana* and most species of *Abra* no lower than 20 ‰). Whilst West and Sparks (1960) suggested that a change in salinity could be observed in their sequence, this is not observed in Unit 2d in this investigation or the research of Brown et al. (1975) and, given the small size of the samples used by Sparks, should be treated with caution.

All of the taxa recorded live in British waters at present so the assemblage is clearly of interglacial character. The presence of *Ovatella myosotis* (*Phytia myosotis* in earlier studies) suggests conditions of some warmth as its modern range only extends as far north as Britain and Denmark (Kerney, 1999). None of the species in this small assemblage have any biostratigraphic significance and thus cannot give any indication of the age of the deposits.

4.2.4 Coleoptera (G. Russell Coope & Nicola J. Whitehouse)

The Unit 2b assemblage from sample BH16 7.74 – 7.79 m (Table 4) contains only ten taxa, including a group of phytophagous beetles that feed on reedy vegetation in a freshwater setting such as *Typha*, *Phragmites*, *Sparganium*, *Carex* and *Eriophorum*. This assemblage provides no evidence of open water or saline conditions. The Coleoptera therefore suggest that the local environment at this time was fen dominated by *Typha* and *Phragmites* which was probably visited by large herbivorous mammals, suggested by the dung beetle *Sphaeridium scarabaeoides* / *lunatum*.

Only two of the species recorded from this samples from Unit 2b could be used for temperature reconstruction using the MCR database. They gave a very wide range of possible palaeotemperature values with 100% overlap of the climatic ranges of the species used. Mean July temperature (TMax) lay within the range +9°C and +26°C and mean January temperature (TMin) within the range –13°C and +13°C. The lowest values of this range and the absence of more thermophilous species may suggest that temperatures during deposition of Unit 2b were lower than those during deposition of Unit 2d.

All the samples from Unit 2d (from Test pits 4, 6 and 7, the top of Borehole 16 and the 1974 sample, Table 4) are very similar. The predominant habitat was extensive reed swamp with *Phragmites*, *Carex*, *Scirpus* and *Typha* with open stationary water and occasional mud banks that were bare of vegetation. There is evidence of the presence of oak trees, ash and hazel bushes (e.g. *Rhynchaenus quercus*, *Curculio venus*, *Hylesinus crenatus* and *H. oleiperda*). *Platypus cylindricus* though probably at some distance from the marshy area. The stag beetle *Lucanus cervus* and the lesser stage beetle *Dorcus parallelipedus* indicate decaying and dying wood in the vicinity. *Scolytus carpini*, which is principally found on *Carpinus betulinus*, implies the presence of this tree (Koch 1992), a species that requires warm conditions. The presence of *Pinus sylvestris* is indicated by *Hylobius abietis* and *Hylastes angustatus*, whilst *Hylurgops palliatus* is found under the bark of all types of conifers including *Abies*, *Larix* and *Pinus* spp. (Bullock 1993).

These assemblages differ from Unit 2b in providing clear evidence of saline habitats, including brackish water and salt marsh species such as *Bembidion normanum* and *Paracymus aeneus*. The assemblage is however dominated by more cosmopolitan species that can tolerate brackishness but do not actively prefer it, such as *Hydroporus*, *Noterus clavicornis*, *Cercyon tristis* and *Enochrus* sp. In summary, the Coleoptera from Unit 2d suggest a salt marsh with pools of eutrophic water in which were accumulations of decomposing plant material. A significant number of dung beetles associated with large grazing animals (e.g. *Caccobius schreberi*, *Onthophagus massai*, *O. verticocornis*, *O. fracticornis*, *Aphodius stictus* and *Aphodius* sp.) together with a diverse forest beetle community also indicates a climax woodland nearby with numerous animal grazers.

There can be little doubt that the coleopteran assemblage from both subunits indicates fully temperate interglacial conditions. The non-British species (e.g. *Bembidion elongatum*, *Oodes gracilis*, *Cybister lateralimarginalis*, *Melanotus niger*, *Throscus* cf *exul*, *Oniticellus fulvus*, *Caccobius schreberi*, *Onthophagus*

massai, and *Heptaulacus* sp.) are all relatively southern with normal northern geographical limits that cross northern France and Germany. The British range of several others only reaches southern England and some of these are extraordinarily rare in this country today (*Bembidion octomaculatum*, *Chlaenius tristis*, *Dimetrius imperialis*, *Hydrovatus cuspidatus*, *Paracumus aeneus*, and *Hydrous caraboides*). The temperature during the summer months was thus a degree or two higher than that in southern England at the present day. Winters may have been no colder than now. Precipitation values cannot be estimated on the basis of this fauna since, though the marshy habitats remained throughout the summer months, the moisture may have been maintained to some extent by the adjacent marine water level. Biostratigraphically, the fauna resembles most closely those that have already been ascribed to the last interglacial (Coope, 2001), particularly in the non-British species described above, including the well-known indicators of this time period *Onthophagus massai* and *Caccobius schreberi*. It also includes a number of distinctive fragments of unidentified species which are not listed in Table 4 but have also been found exclusively in faunas of this age. There are also similarities to the fauna reported from the sequence at Hackney Downs that was initially dated to the last interglacial (Gibbard, 1994) but more recently suggested to date from an interglacial that correlates with MIS 9 (Green et al., 2006). Key species that are present here at Stone Point, also at Hackney Downs (Green et al., 2006) and in many last interglacial sequences (Coope, 2001) include *Bembidion elongatum* and *Caccobius schreberi*. In addition *Onthophagus massai* is present, which is reported from only a few Ipswichian Interglacial deposits. Note that there is some taxonomic debate about this species, outlined in full in Langford et al. (2017), but we retain it here because it represents a specific morphotype that has biostratigraphic significance.

Forty-four coleopteran species from all the samples from Unit 2d (Table 4) were used to obtain the temperature reconstruction using the MCR database, making it very robust. They give the following palaeotemperature values with 100% overlap of the climatic ranges of the species used: mean July temperature lay within the range +17°C and +18°C; mean January temperature lay within the range -2°C and 0°C. Because several of the more southern species, which today live in central and southern Europe (e.g. *B. elongatum*, *O. massai*) are not present in the MCR database, this may be a conservative temperature estimate. These estimates are very similar to palaeotemperature estimates from Deeping St James (Keen et al., 1999 - TMax 17-18°C, TMin 0 to 4°C) and Itteringham (Beesley, 1988 - TMax 17-19°C, TMin 1 to -4°C).

4.2.5. Ostracods and foraminifera (John E. Whittaker)

Samples were taken from the full depth of the sequence from Test pits 4b and 4d, Test pit 7 and Boreholes 13 and 16. No ostracods or foraminifera were preserved from Unit 2b. The foraminifera and ostracods from Unit 2c (Table 5) are very low diversity brackish, inner estuarine assemblages; those of intertidal mudflats and creeks. There are no marine or even outer estuarine species present so the site must have been much too far from the then Solent Estuary mouth for them even to be brought in on the tide or in periods of storm. There are however a few freshwater ostracods, which suggest that the site was at that time close enough to freshwater ecosystems for fossils to be transported downstream from them.

Unit 2d has a different assemblage from Unit 2c. The lower parts of test pit 7, borehole 13 and borehole 16 contain a high number of intertidal foraminiferal species such as *Haynesina germanica* and *Elphidium williamsoni* in test pit 7, although not in borehole 13, which is dominated by *Ammonia aberdoveyensis* and *Elphidium waddense*. Also present in both is the euryhaline estuarine ostracod *Leptocythere castanea*, although the sequence is dominated by abundant *Cyprideis torosa* (all non-noded). This part of the sequence is therefore interpreted as a tidal (brackish) mudflat. There is no freshwater influence, neither is there indication of salt-marsh nearby. The salinity was also clearly above c. 6‰ as evidence by the exclusively non-noded populations of *Cyprideis torosa*.

In the upper parts of Unit 2d (test pits 4b and 4d, top of test pit 7) the dominant foraminifera are *Ammonia aberdoveyensis*, *A. limnetes* and *Elphidium waddense*, all of which indicate brackish conditions, in a tidal river or estuary, with *E. waddense* and the agglutinating saltmarsh species, *Trochammina inflata* indicating

low saltmarsh. The dominant ostracod is *Cyprideis torosa*, which is represented by a full population age structure from adults to the smallest juveniles, so is definitely *in situ*. The populations are almost entirely smooth, although some of the specimens have small nodes which may indicate that the salinity is at or near a point where nodding (given other suitable ecological conditions being present) can develop; i.e. c. 5‰ (see Meisch, 2000). This species is indicative of sheltered creeks, as is *Leptocythere porcellanea*, whereas the rarer *Loxoconcha elliptica* is usually found in more open intertidal flats. Non-marine ostracods are rare, but present, although both *Candona* sp. and *Heterocypris salina* are able to tolerate low salinities in coastal pools. The environment represented in the upper parts of Unit 2d is interpreted as an area of low saltmarsh, cut by creeks.

No indication of age or climatic significance can be deduced from the microfaunas, since all the species are still living in Britain and indeed could readily be collected from similar environments in the area today.

4.2.6 Diatoms (Nigel G. Cameron)

Diatoms from borehole 16 (Figures 5 and 6) are poorly preserved, with a high degree of diatom valve breakage and silica dissolution. In Unit 2b, the diatoms identifiable to species level (including *Diploneis didyma*, *Nitzschia granulate*, *Achnanthes brevipes* and *Paralia sulcata*) indicate that there were tidal conditions in the sedimentary environment. Overlying this in Unit 2c, dominant diatoms are marine (almost 70% of the total are polyhalobous diatoms and the planktonic species *Paralia sulcata* is particularly common). Brackish water, mesohalobous diatoms comprise a further 20% of the assemblage, many of which (*Caloneis westii*, *Diploneis didyma*, *Nitzschia compressa* and *Nitzschia navicularis*) are found in mudflats. The diatom assemblage from Unit 2c thus represents full tidal conditions.

The diatom assemblage from the base of Unit 2d (745-746 cm) shows an increase in both diatom numbers and species diversity from Unit 2c. Mesohalobous diatoms increase to almost 75% of the total, including particularly commonly (c. 20%) the littoral species *Rhopalodia musculus*. A number of oligohalobous indifferent (freshwater) taxa are present including *Cocconeis placetula* and *Epithemia* spp. These changes reflect a decrease in salinity. This, however, is shortlived as higher in Unit 2d (529-530 cm) oligohalobous species drop again, with an assemblage comprising similar proportions of polyhalobous (over 40%) and mesohalobous diatoms (almost 45%) (Figures 5 and 6) and many marine taxa including *Paralia sulcata*. A few fragmented marine species are preserved from 215-216 cm depth showing continued brackish conditions. All samples above this were barren.

4.3. Trace-element and stable-isotope determinations of ostracod shells (Jonathan Holmes)

It was clear from field discussions following the publication of Briant et al. (2009) that the salinity signal of this sequence was important and not yet comprehensively demonstrated. Therefore 11 isotopic determinations were undertaken on samples from test pits 4b, 4d and 7 and borehole 13. Mg/Ca and Sr/Ca in ostracod shells (Figure 7) are positively correlated with the trace-metal to Ca in the water in which the shells calcified and, for Mg, with water temperature. Trace-element partitioning between ostracod shell and water can be described using species- or genus-specific partition coefficients (KD[M] values, where $KD[M] = M/C_{shell}/M/C_{water}$, and M is either Mg or Sr). Whilst not without problems (e.g. Dettman and Dwyer, 2012), KD values can be used in some circumstances to reconstruct quantitatively the M/Ca of water. In marginal-marine waters, highly non-linear variations in water M/Ca and salinity arise from the mixing of sea-water with water from meteoric sources. This raises the possibility of using trace-element determinations to reconstruct both water composition and temperature (Holmes and De Deckker, 2012). This approach has been used successfully for trace-element determinations of *C. torosa* in marginal-marine settings (e.g. Holmes and De Deckker, 2015). De Deckker et al. (1999) have further shown that the Mg/Ca of *C. torosa* shells can be used to reconstruct water temperature using the equation $T\text{ }^{\circ}\text{C} = 2.69 +$

5230(Mg/Ca_{shell}/Mg/Ca_{water}). Clearly, this requires independent knowledge of Mg/Ca_{water}. For the material from Stone Point, we estimate the Mg/Ca of water using Sr/Ca_{water} estimates, derived from the Sr/Ca of each shell and assuming KD[Sr](*Cyprideis*) of 0.47 (Holmes and De Deckker, 2015), and a simple mixing model for Stone Point water based on seawater and chalk-derived groundwater (Figure 8). While somewhat oversimplified, this probably yields reasonable values.

The $\delta^{18}\text{O}$ value of ostracod shells is determined by water isotope composition and water temperature. Ostracod shells are generally offset from isotopic equilibrium: for *C. torosa*, the magnitude of the offset is poorly constrained, but probably around +0.8 ‰ (Holmes and De Deckker, 2015). The $\delta^{18}\text{O}$ of water in marginal-marine waters is determined primarily by mixing of seawater and meteoric water, but unlike for trace-element to Ca ratios, the mixing line is linear. For carbon isotopes, the $\delta^{13}\text{C}$ value of ostracod shells is determined primarily by the $\delta^{13}\text{C}$ of dissolved inorganic carbon (DIC). Although this can be controlled by a number of factors, in marginal-marine waters it is often a function primarily of the relative balance of marine and non-marine water, since seawater and meteoric water usually have contrasting $\delta^{13}\text{C}_{\text{DIC}}$ values. Carbon isotopes therefore provide a complementary line of evidence for mixing of different water types in such settings.

Reconstructed Sr/Ca water values for Stone Point material range from 0.0051 to 0.0075 (Figure 7): although quite variable, these represent values that are likely to be lower than that for fully-marine water (assumed to be close to present-day values i.e. 0.0088). Use of the mixing model in Figure 8 suggests that this equates to around 7 to 13% seawater in the mixture, or a salinity of 2.5 to 4.6 psu, and Mg/Ca of between 4.62 and 4.73. We note that these reconstructions carry quite large uncertainties owing to uncertainties in the KD values and in the water mixing model: however, they probably provide a reasonable first order estimate of water composition. The reconstructed Sr/Ca_{water} and hence salinity values are likely to be minimum values – Sr/Ca_{water}, and hence Sr/Ca_{ostracod}, becomes quite insensitive to further increases in salinity, as the mixing model (Figure 8) shows. However, salinity values below those quoted would lead to a dramatic reduction in the Sr/Ca_{water}, and hence Sr/Ca_{ostracod}. We note that reconstructed Sr/Ca and salinity values do not vary dramatically up sequence within Unit 2d and that the inferred water composition was always brackish, never fresh nor fully marine

Weak positive correlation between Mg/Ca and Sr/Ca in the Stone Point ostracods suggests that some of the variability in Mg/Ca may be related to changes in water composition. We therefore use the inferred % seawater values and the mixing model in Figure 8 to infer water Mg/Ca in the Mg/Ca palaeotemperature equation in order to reconstruct water temperature. This yields average temperature values for individual stratigraphic levels at Stone Point sequence of 13.1 and 20.4°C (Figure 9). Given the life-history of *C. torosa*, these values likely represent spring or late summer/autumn temperature (Heip, 1976a, b). The estimates carry additional but un-quantified uncertainty from uncertainties in the Mg/Ca_{water} reconstructions and so must be viewed with caution.

For oxygen isotopes, we have fewer determinations and it should be noted that these were not undertaken on the same shells as the trace-element measurements. Use of the Mg/Ca-inferred temperatures quoted above and a vital offset of +0.8 ‰ confirms the suggestion, based on trace elements, that the Stone Point water was a mixture of marine (assumed $\delta^{18}\text{O} = 0$ ‰) and meteoric (assumed $\delta^{18}\text{O} = -6.5$ ‰ based on modern values: Darling et al., 2003) sources although calculations suggest a rather greater proportion of non-marine water in the mixture. However, the calculations carry large uncertainties owing to uncertainties in the $\delta^{18}\text{O}$ values of the endmembers, in the Mg/Ca temperature reconstructions (especially since these do not relate to the exact same shells as those used for isotope analysis) and in the vital offset, so differences may not actually be significant. Lower $\delta^{18}\text{O}$ values in the lowermost three levels analysed at Stone Point are consistent with an increased freshwater input and hence lower salinity, although we note that these levels are not associated with lower M/Ca values, indicating that any reduction in salinity was not sufficient to lower the M/Ca ratios of the

water. The overall range of $\delta^{18}\text{O}$ values (3 ‰) in *Cyprideis* is too large to be explained by temperature change alone (which would equate to about 12°C temperature range), however, and must in part be due to changes in freshwater input to the mixture. Weak positive correlation of $\delta^{13}\text{C}$ with $\delta^{18}\text{O}$ lends support to our suggestion that changes in the isotopes are related to variable freshwater input to the mixture.

Overall, the ostracod geochemical determinations suggest that the environment represented by Unit 2d was brackish, with no evidence of fully marine or fully freshwater conditions and salinity that was closer to the freshwater rather than the marine end of the brackish range. There is some evidence for slightly fresher conditions nearer the base of the sequence analysed, although this is evident only in the stable isotope data, not the trace elements. We caution that the reconstructions carry large uncertainties.

4.3 Geochronology (Jean-Luc Schwenninger and Kirsty E.H. Penkman)

Five optically-stimulated luminescence (OSL) samples from Units 1 and 4 have previously been reported in Briant *et al.* (2006). Age estimates from Unit 1 (Lepe Lower Gravel) (LEPE03-01, 02, 03, 04) span 230 to 130 ka (MIS 7d-5e, Table 3), broadly coincident with the cold stage immediately preceding the last interglacial (i.e. MIS 6). Error bars for these age estimates are relatively small, however, meaning that these age estimates do not overlap. These differences are discussed in Briant *et al.* (2006) and probably reflect both inter-aliquot variability and difficulties in estimating long-term water content and overburden history because of proximity to present-day sea level. It was only possible to take one sample from Unit 4 (LEPE03-05) because this unit is less sand-rich than Unit 1. The OSL age of this is between 72 and 58 ka (MIS 4-3), post-dating the deposition of Unit 1. It should be noted that age estimates from Unit 1 overlap MIS 7d, which might suggest that Unit 2 could date from the penultimate interglacial, particularly if the terrestrial expression of the MIS 7 interglacial is correlated with one of the later substages (i.e. MIS 7a or 7c). This age for Unit 2 is less likely if the terrestrial interglacial correlated with either or both of MIS 7c or 7e, as suggested by Candy and Schreve (2007). Furthermore, two of the four OSL ages post-date MIS 7. For these reasons, we consider a penultimate interglacial (MIS 7) age less likely and suggest instead that the Stone Point organic deposits are more likely to date from the last interglacial (Ipswichian, MIS 5e) than from MIS 7.

These previously-reported OSL ages conflict with previous interpretations of the timing of deposition of the overlying Unit 5. The TL dates of c. 20 ka and 98/120 ka reported by Parks (1990; Parks and Rendell, 1992) are older than the OSL age from Unit 4. However, TL dates on sediment are problematic because of the almost certainty of partial bleaching of this light insensitive signal. Because of this uncertainty about the age of Unit 5 following discussion in the field after publication of Briant *et al.* (2009), a further four OSL samples were taken from Section 1 in 2010. As can be seen from Table 7, two of the samples from Unit 5 (LEP10-02, -04; X4103, X4105) yielded ages in MIS 4-3, centred around 40-50 ka, only a little younger and partially overlapping the age estimate from Unit 4. The other two samples (LEP10-01, -03; X4102, X4104) yielded anomalously young ages. For this reason, after measurement of an initial 12 aliquots for each sample, a further 12 aliquots were measured only for LEP10-02 and -04 (X4103, X4105) since these seemed to be more tightly clustered.

Figure 10 shows the D_e distributions for single aliquot measurements on each sample, including a value for skewness to aid detection of bioturbation (Bateman *et al.*, 2007). Whilst skewness values are relatively low, only X4103 has an approximately normal distribution, and even this has a significant tail of older dates. Most striking is the large number of very low D_e 's in X4102 and 4104. The most likely explanation is that these samples, so close to the ground surface, have been affected by bioturbation. This could have occurred during either soil formation or burrowing by sand wasps or bees (Sphecidae) (see Table 1). The very young ages suggest incorporation of almost zero-age material. Although care was taken during sampling to avoid fresh burrows, it is possible that older burrows will have collapsed and therefore have incorporated very recently bleached material into the samples. Bee bioturbation may have also caused older material to be incorporated from the underlying gravel. This evidence further suggests that previous TL ages from this unit should be

disregarded, as these were produced using a multiple aliquot protocol which produced a single age estimate from results from multiple aliquots that does not allow scatter to be determined. Given the scatter between aliquots observed here, the previous TL dates are even less likely to reflect a true age estimate.

These difficulties mean that it is hard to assign an age to Unit 5. However, on the basis of the clustering of De's around 100 Gy in X4103 and (to a lesser extent) X4105, it seems likely that it either dates from or postdates MIS 4-3. This strengthens the single age estimate previously reported from Unit 4 and thus the suggestion that the interglacial deposits date from MIS 5e.

Because the OSL dating was unable to provide an age estimate for the interglacial silts directly, we sought an alternative method to provide such an age estimate, as part of the process of seeking to reconstruct the full record of sea level at this location. As discussed above, multiple fossil groups show evidence for freshwater influence from Units 2b and 2c. Therefore when *Bithynia tentaculata* opercula were found from a sample within Unit 2c, it seemed likely that this was also part of the evidence for freshwater influence in this part of the sequence, even if not directly *in situ*. (As discussed below, it seems likely that none of the freshwater fossils represent individuals that were living at this exact location, since they are a minority of the assemblage in every case). As such, it seemed likely that these opercula could provide a robust age for the base of this sequence. Even if they had been reworked from earlier deposits, they would provide a maximum age estimate for comparison with OSL age estimates.

For this reason, AAR analyses were undertaken on two small individual *Bithynia tentaculata* opercula from Unit 2c within borehole 16 between 754 and 756 cm depth (NEaer 3312-3313, Figure 12). The sample size for 3313 was very small, with concentrations similar to the analytical level of detection, so the data from this sample (Table 8) should be considered with caution, although comparison of free and total hydrolysed fractions for both samples suggested closed system behaviour. The range of data for British sites has been compared to the Lepe dataset (Figure 11), and the Lepe samples have Ala amino acid ratios that are similar to sites correlated with the penultimate interglacial (MIS 7) (Penkman *et al.*, 2011), although the small sample size precludes further resolution at this stage.

There is no analytical evidence for error in the AAR data. Therefore the conflicting age estimates from the AAR and OSL must have a different cause. It should firstly be noted that the OSL samples from Unit 1 were taken beneath a thinner part of the Unit 2 sequence, further onshore, so cannot be directly compared with the AAR from the base of borehole 16. Although the multiple boreholes shown in Figure 2 and the continuity of the vegetation succession in the pollen record both strongly suggest that the sediments in borehole 16 are a continuous sequence and contemporary with thinner sequences further onshore, there is a small possibility that the Unit 2c sediments sampled for AAR represent a remnant of older deposits. The full sequence cannot plausibly be assigned to the penultimate interglacial (MIS 7) because of both the OSL age estimates from Unit 1 and the implausibility of a full climatic cycle hiatus between the top of Unit 2 / Unit 3 and Unit 4. We therefore suggest that the AAR results provide a maximum age estimate for this sequence, firmly constraining it to the more recent part of the Pleistocene. In this interpretation, instead of transport downstream within the contemporary estuary as with freshwater evidence from other fossil groups, these samples must have been reworked from an earlier deposit. Indeed, they are very small and found within a sand lens rather than in the finer-grained material, which further supports the reworking interpretation.

5. Discussion

5.1 Age of the sequence

Biostratigraphic indications of age from the pollen assemblages are limited, although the presence of *Carpinus* might indicate an Ipswichian (last) interglacial age. More conclusive are the Coleoptera, which resemble most closely those assemblages that have already been ascribed to the last interglacial (Coope, 2001). This resemblance includes several significant “non-British” species (e.g. *Bembidion elongatum*,

Caccobius schreberi and *Onthophagus massai*) none of which have yet been found in penultimate interglacial assemblages. It also includes distinctive fragments of unidentified species found exclusively in last interglacial faunas (Coope, 2001) and rare southern English species including *Bembidion octomaculatum*, *Paracumus aeneus* and *Hydrous caraboides*.

As discussed above, the dating is not conclusive from this sequence and the AAR and OSL conflict. However, the balance of probability is that the most likely age for this sequence is the Ipswichian (last) interglacial, particularly given the biostratigraphic evidence above. Treating the age estimate from AAR analyses (penultimate interglacial) as a maximum also suggests that the sequence is relatively young. Freshwater species such as the opercula used for AAR analysis are likely to have been transported into the sequence from upstream, but this result suggests that there was also scouring of previously deposited material during transgression. It might also indicate an erosional discontinuity within the interglacial sequence that is undetectable because of both the limited exposure inherent in borehole-based investigations and the sedimentological and faunal similarity of most estuarine interglacial material. This latter explanation seems less likely because of the OSL age from underlying gravels. It therefore seems most likely that this sequence is of Ipswichian (last interglacial, MIS 5e) age and that the AAR correlation represents a maximum age.

5.2 Timing of sea level rise during the Ipswichian (last) interglacial

The combination of fossil groups present in this sequence enables determination of the timing of sea level rise within the last interglacial in relation to the establishment of forest. A clear interglacial development is seen in the vegetation, with Units 2b and 2c dominated by grass and pine (IpI). Oak and birch then occur from the very base of Unit 2d upwards, with changing percentages of other species indicative of a development from IpIIa to IpIIb. The assemblages throughout this unit show mixed-oak woodland, as also reported by West and Sparks (1960) and Brown *et al.* (1975). Determining the timing of sea level rise recorded in this sequence is more complicated. Figure 12 summarises the salinity signal from the full sequence, integrating records from all the test pit and boreholes investigated by PASHCC and the West and Sparks (1960) sequence.

It is clear from the summary in Figure 12 that even the lower parts of the sequence have a strong brackish signal. Freshwater species are slightly more significant in Units 2b and 2c. For example, fossil coleopteran assemblages from Unit 2b are interpreted as representing a freshwater fen and two opercula of the species *Bithynia tentaculata* used for AAR analysis from Unit 2c (755 cm, borehole 16) are the only freshwater evidence in the mollusc sequence from borehole 16 (Dr Richard Preece, *personal communication*). In Unit 2d, the sequence is again predominantly brackish, although here too some freshwater elements occur. For example, terrestrial plant macrofossils include wood, buds, cupules and fruit of *Quercus robur*, and fruit of *Acer* reported by Brown *et al.* (1975). In the peat beds near the top of Unit 2d, saltmarsh and freshwater plant macrofossils are equally frequent, with freshwater species including *Carex cf. riparia*, *Carex cf. rostrata*, *Hydrocotyle vulgaris*, *Lemna* sp., *Lycopus europaeus*, *Menyanthes trifoliata*, *Ranunculus sceleratus* and *Sparganium* sp. (Brown *et al.*, 1975).

The new isotopic determinations reported in this paper enable us to quantify the salinity during formation of Unit 2d. The ostracod trace-element data support the existence of brackish water, with a slight trend towards lower Mg/Ca and Sr/Ca values up sequence (Figure 7), although within-level variability is always relatively high. Calculations with a simple mixing model (Figure 8) suggest that the water contained up to about 13% seawater, giving a salinity value of up to about 4.6 psu. The overall picture gained here therefore is one of early sea level rise. Units 2b and 2bc (IpI) are defined as mixed and 2d (IpIIa and IpIIb) as brackish (Figure 13). The mixing of species in this sequence suggest that the site occupied a position mid-estuary where transport of individuals from both up and downstream was common. Whilst it is possible that this, and the switching between minerogenic and organic sediment accumulation seen in Unit 2d can be associated with fluctuating sea levels, as in the Holocene (Long *et al.*, 2000), it is also possible that local sediment budgets are more important in this case (e.g. Bates and Whittaker, 2004). Given the proximity of the site to the edge

of the likely floodplain, local factors will have played significant roles in sediment accumulation, and input from freshwater and brackish sources will have varied as channels switched across the inundated area. Differences in interpretation between the different fossil groups may reflect different taphonomic pathways or difficulties in sampling directly comparable material from boreholes. It is possible that the final slight freshening towards the top of Unit 2d (peat beds) is a response to a decrease in accommodation space, as in sedimentary sequences infilling many of our estuaries at the present time (e.g. Devoy, 1979).

The evidence from this sequence is important, as discussed above, because it is the longest fossiliferous record of sea level change for the last interglacial in the Channel region (sequences in France are more fragmentary and also dated to previous interglacials – e.g. Antoine et al., 2007). Placing it in the context of other relevant but shorter sequences along the Solent seaway confirms the interpretation that Lepe is in a mid-estuary position (Figure 13), as they show a west to east transition from freshwater to brackish. To the far west, early interglacial (birch-pine, IpI) deposits with freshwater affinities occur at –3.9 to –5.3 m O.D. depth c. 17 km upstream at Pennington Marshes (Allen *et al.*, 1996). Closer, c. 5 km upstream, a slightly older interglacial vegetation sequence (IpII/IpIII) is preserved at St Leonards Farm at c. 0.1–1.8 m O.D. (Briant *et al.*, 2013). This sequence contains both freshwater and marine fossils. In addition, to the far east, c. 25 km downstream is a fully brackish sequence at Bembridge Foreland from c. 4–6 m O.D. (Preece et al., 1990).

A rapid and early rise in sea level is also seen in global sea level records (e.g. Siddell et al., 2005) and in the well-dated Dutch record where the initial rise is observed in E2, equivalent to IpIb (e.g. Long et al., 2015). This is likely to be due to rapid retreat of the Saalian ice sheet, possibly in response to early peak warmth in the last interglacial, as reported by Langford et al. (2017), although all other British sequences report peak warmth in IpIb (as far as can be determined given how fragmentary they are – Candy et al., 2016). MCR temperature reconstructions from this sequence suggest summer temperatures of c. 9–26°C during deposition of Unit 2b (IpI) and c. 17–18°C during deposition of Unit 2d (IpIIa to IpIb). Water temperature reconstructions from the Stone Point organic deposits from Mg/Ca in shells of the ostracod *Cyprideis torosa* are $17 \pm 3^\circ\text{C}$ for the upper parts of the sequence. There is some suggestion of higher temperatures in the lower part of the sequence (–3 to –5 m OD: $18 \pm 3^\circ\text{C}$) and lower temperatures in the upper part (above –2.22 m OD: $15 \pm 2^\circ\text{C}$). However, the uncertainties in the temperature reconstructions are poorly constrained and so the apparent trend may not be real, although we note that the increase in $\delta^{18}\text{O}$ values in the upper part of the sequence with no accompanying trace-element data to support an increase in salinity is consistent with lower water temperature. These are similar to mean July air temperatures reconstructed from most Ipswichian sequences of 18°C (Candy et al., 2016), but lower than the mean July temperatures reported from Trafalgar Square (c. 20–21°C) and Whittlesey (c. 19–23°C, Langford et al., 2017).

This rapid sea level rise has implications for hominin movement from the continent to Britain. Ashton and Lewis (2002) talk about the presence of ‘windows of opportunity’ for immigration to Britain between ice melting and sea level rising. The early sea level rise recorded here makes the window small for the last interglacial, exacerbated further by the likely final breaching of the Straits of Dover (Gupta et al., 2017). Our findings therefore strengthen this proposed explanation for hominin absence in the last interglacial. However, it should be noted that last interglacial deposits, whilst lacking in hominins, do contain an abundance of warm climate taxa (i.e. hippo, straight-tusked elephant etc. – Sutcliffe, 1995). Therefore sea level rise did not occur so fast that it prevented these animals from reaching Britain. There is tantalising evidence further east, adjacent to the North Sea basin (Langford et al., 2017) that Britain was already very warm by IpI. It is possible that the presence of a warm climate fauna is a response to this early warming, since the ‘windows of opportunity’ suggested by Ashton and Lewis (2002) also relate to warming. If so, a plausible explanation for the different migration patterns of these fauna and hominins would be required. Ashton and Lewis (2002) note that sparse hominin sites from the whole of northwest Europe in the last interglacial might suggest that humans were present further east, having adapted to hunting on the mammoth-steppe. This might explain why a diverse range of warm climate fauna that are not known to have been hunted extensively by hominins arrived in Britain but hominins did not.

5.3 Stratigraphic implications of interglacial sedimentation in estuaries

The deposition of Transgressive Systems Tract deposits over a significantly time transgressive erosional surface caused by previous incision during base level fall is a central part of sequence stratigraphic principles (e.g. Posamentier and Vail, 1988; Posamentier et al., 1988). There has been significant debate about how far up-valley this relationship should be expected to be observed (e.g. Leeder and Stewart, 1996; Blum and Törnqvist, 2000). However, the Lepe site is so close to past shorelines that this conceptual model can usefully be used here.

Gibbard (1994) has argued that the Lower Thames estuarine interglacial sequences show this onlapping onto older terrace deposits. In this model, as transgression progressed, sediment was progressively deposited over altitudinally higher and higher deposits. Gibbard (1994) argues that sedimentation would have been controlled by sea level, with its rate controlled by the volume of sediment supplied by the river. This model conflicts with vertebrate-based biostratigraphic models (Schreve, 2001) that ascribe sequences at various locations on the terrace level above that which contains the last interglacial deposits of Trafalgar Square to the penultimate interglacial. The Gibbard (1994) model instead assigns interglacial deposits overlying both terrace levels (and indeed several higher ones) all to the last interglacial. The Gibbard (1994) model has conceptual appeal and does make sense of the fact that frequently these extensive estuarine deposits are not overlain by further fluvial deposits. Furthermore, the Holocene deposits in the Lower Thames demonstrably do overlie two different gravel aggradations – the Shepperton Gravel throughout and the higher East Mucking / Kempton Park Gravel in places.

Such an onlapping model is harder to apply in the Solent, however, because two of the four sequences summarised in Figure 13 (Pennington and Lepe / Stone Point) are overlain by fluvial gravels at significantly different elevations. These were mapped by Allen and Gibbard (1993) as separate gravel bodies. Westaway et al. (2006) failed to either confirm or deny this difference, concentrating instead on the higher and more extensive deposits. Hatch (2013; et al., submitted) tackled the many disparities between these two stratigraphic schemes by a comprehensive re-examination of boreholes in the region and additional geophysical data using modern borehole comparison software. He reassigned the gravels of Units 1 and 4 of this study (previously Lepe Lower and Upper Gravels) to the Milford on Sea Gravel and confirmed the gravels above and below the Pennington interglacial deposits as a separate aggradation, extremely geographically confined. It is therefore possible that last interglacial deposits in the Solent were deposited over a time transgressive surface. If this were so, then at the start of the interglacial the river channel was at the altitude of the Pennington Lower Gravel, later overlapping the lower gravel (Unit 1) at Lepe. At Pennington, deposition occurred in a freshwater environment, at least during IpI, which is the only part of the interglacial from which we have evidence preserved. Further downstream, at Lepe, the Stone Point organic deposits were laid down in a mid-estuary situation. The valley continued to fill, onlapping Unit 1 and reaching a maximum altitude of c. 1 m O.D. in Ip IIb. No later deposition is recorded here, but upstream at St Leonards Farm the Ip II/III transition is possibly preserved in a proto-Beaulieu River, which did not then deposit further gravel over the deposits. It is also recorded downstream in the more open setting of Bembridge Foreland, adjacent to a raised beach deposit (Preece et al., 1990; Figure 13). Once sea levels fell again, incision took place at both Pennington and Lepe. The fluvial deposition following this incision is the part of the sequence that fits this model least well, because deposits at noticeably different elevations contain OSL age estimates that are very similar, particularly LEPE03-05 at 66 ± 7 ka and PENN03-06 at 53 ± 6 ka (Briant et al., 2006a). There is no obvious mechanism for this at a time of stable, low sea level. Nonetheless, it is clear from the discussion above that there is significant potential for interglacial estuarine deposits to have a confusing or problematic relationship to their associated stratigraphy. Therefore they should be used with caution to provide tie-points for terrace sequences.

6. Conclusion

We have reported new data from the longest fossiliferous last interglacial sequence in the Channel region – thin section analysis of Unit 3, new MCR analysis from coleoptera, isotopic determinations on ostracod shells from Unit 2d, new OSL ages on Unit 5 and AAR analyses on Unit 2c. These show early sea level rise, although no early warming, starting during the pre-temperate vegetation zone IpI which is characterised by birch-pine assemblages. This agrees with patterns observed in the Netherlands and suggests that the ‘window of opportunity’ for human colonisation of Britain at the start of the last interglacial may indeed have been very small (cf Ashton and Lewis, 2002), particularly given the likely final breach of the Straits of Dover at this time (Gupta et al., 2017).

The stratigraphic linkage of the last interglacial deposits in the Solent seaway to fluvial terrace deposits at two different altitudes requires us to rethink our understanding of such relationships. It is clear that when interglacial deposits are estuarine in affinity, they may onlap older deposits and have a time transgressive lower contact. Thus we should be cautious about using them as tie-points on which to build a terrace chronology.

7. References

- Adamiec, G. and Aitken, M.J., 1998. Dose-rate conversion factors: update. *Ancient TL*, 16(2), pp.37-50.
- Allen, L.G. and Gibbard, P.L. (1993) Pleistocene evolution of the Solent River of southern England. *Quaternary Science Reviews*, 12, 503-28.
- Allen, L.G., Gibbard, P.L., Pettit, M.E., Preece, R.C. and Robinson, J.E. (1996) Late Pleistocene interglacial deposits at Pennington Marshes, Lymington, Hampshire, southern England. *Proceedings of the Geologists' Association*, 107, 39-50.
- Antoine, P., Coutard, J.-P., Gibbard, P.L., Hallegouet, B., Lautridou, J.-P. and Ozouf, J.-C. (2003) The Pleistocene rivers of the English Channel region. *Journal of Quaternary Science* 18, 227-243.
- Antoine, P., Lozouet, N.L., Chaussé, C., Lautridou, J.P., Pastre, J.F., Auguste, P., Bahain, J.J., Falguères, C. and Galehb, B., 2007. Pleistocene fluvial terraces from northern France (Seine, Yonne, Somme): synthesis, and new results from interglacial deposits. *Quaternary Science Reviews*, 26(22), pp.2701-2723.
- Ashton, N. and Lewis, S., 2002. Deserted Britain: declining populations in the British late Middle Pleistocene. *Antiquity*, 76(292), pp.388-396.
- Atkinson, T.C., Briffa, K.R. and Coope, G.R., 1987. Seasonal temperatures in Britain during the past 22,000 years, reconstructed using beetle remains. *Nature*, 325(6105), p.587.
- Banerjee, D., Murray, A.S., Bøtter-Jensen, L. and Lang, A., 2001. Equivalent dose estimation using a single aliquot of polymineral fine grains. *Radiation Measurements*, 33(1), pp.73-94.
- Bassinot, F.C., Labeyrie, L.D., Vincent, E., Quidelleur, X., Shackleton, N.J. and Lancelot, Y., 1994. The astronomical theory of climate and the age of the Brunhes-Matuyama magnetic reversal. *Earth and Planetary Science Letters*, 126(1-3), pp.91-108.
- Bateman, M.D., Boulter, C.H., Carr, A.S., Frederick, C.D., Peter, D. and Wilder, M., 2007. Preserving the palaeoenvironmental record in drylands: bioturbation and its significance for luminescence-derived chronologies. *Sedimentary Geology*, 195(1), pp.5-19.

- Bates, M.R. and Whittaker, K. 2004. Landscape evolution in the Lower Thames Valley: implications of the archaeology of the earlier Holocene period. In: Cotton, J. and Field, D. (eds.) *Towards a New Stone Age: aspects of the Neolithic in south-east England*, p.50-70. CBA Research Report RR 137. Council for British Archaeology: York.
- Bates, M.R., Briant, R.M., Rhodes, E.J., Schwenninger, J-L. & Whittaker, J.E. 2010. A new chronological framework for Middle and Upper Pleistocene landscape evolution in the Sussex/Hampshire Coastal Corridor. *Proceedings of the Geologists' Association* 121, 369-392.
- Battarbee, R.W., 1988. The use of diatom analysis in archaeology: a review. *Journal of Archaeological Science*, 15(6), pp.621-644.
- Beesley, A.R., 1988. *The Climatic and Environmental Significance of an Interglacial Coleopterous Fauna from Ippinge Norfolk* (Doctoral dissertation, University of Birmingham).
- Blum, M.D. and Törnqvist, T.E., 2000. Fluvial responses to climate and sea-level change: a review and look forward. *Sedimentology*, 47(s1), pp.2-48.
- Briant, R.M., Bates, M.R., Schwenninger, J-L & Wenban-Smith, F.F. 2006a. A long optically-stimulated luminescence dated Middle to Late Pleistocene fluvial sequence from the western Solent Basin, southern England. *Journal of Quaternary Science* 21, 507-523.
- Briant, R.M., Bates, M.R., Boreham, S., Wenban-Smith, F.F. & Whittaker, J. 2006b. Re-investigation of interglacial sediments at Stone Point, Lepe Country Park, Hampshire. *Quaternary Newsletter* 108, 43-51.
- Briant, R.M., Bates, M.R., Boreham, S., Cameron, N.G., Coope, G.R., Field, M.H., Keen, D.H., Simons, R.M.J., Schwenninger, J-L, Wenban-Smith, F.F. and Whittaker, J.E., 2009. Gravels and interglacial sediments at Stone Point Site of Special Scientific Interest, Lepe Country Park, Hampshire. In: Briant, R.M., Bates, M.R., Hosfield, R.T. and Wenban-Smith, F.F. (2009). *The Quaternary of the Solent Basin and West Sussex Raised Beaches*. Field Guide, Quaternary Research Association, p. 171-188.
- Briant, R.M., Bates, M.R., Boreham, S., Coope, G.R., Field, M.H., Wenban-Smith, F.F. and Whittaker, J.E. (2013). Palaeoenvironmental reconstruction from a decalcified interglacial sequence in the former Solent river system at St Leonard's Farm, Hampshire, England. *Quaternary Newsletter* 130, 23-40.
- Bridgland, D.R. (2001) The Pleistocene evolution and Palaeolithic occupation of the Solent River in Wenban-Smith, F.F. and Hosfield, R.T. (eds.), *Palaeolithic archaeology of the Solent River*. Lithic Studies Society Occasional Paper 7, 15-25, Lithic Studies Society, British Museum, London, 111pp
- Bridgland, D.R. and Schreve, D.C. (2001) River terrace formation in synchrony with long-term climatic fluctuation: supporting mammalian evidence from southern Britain. In, Maddy, D., Macklin, M. and Woodward, J. (eds). *River Basin Sediment Systems: Archives of Environmental Change*, 229-248, Balkema, Rotterdam.
- Brown, R.C., Gilbertson, D.D., Green, C.P. and Keen, D.H. (1975) Stratigraphy and environmental significance of Pleistocene deposits at Stone, Hampshire. *Proceedings of the Geologists' Association*, 86, 349-363.
- Buckland, P. and Buckland, P. 2012. *Bugs Coleopteran Ecology Package*, <http://www.bugscep.com>

- Candy, I. and Schreve, D., 2007. Land–sea correlation of Middle Pleistocene temperate sub-stages using high-precision uranium-series dating of tufa deposits from southern England. *Quaternary Science Reviews*, 26, 1223–1235.
- Candy, I., White, T.S. and Elias, S., 2016. How warm was Britain during the Last Interglacial? A critical review of Ipswichian (MIS 5e) palaeotemperature reconstructions. *Journal of Quaternary Science*, 31(8), pp.857–868.
- Coope, G.R., 1986. Coleoptera analysis. *Handbook of Holocene palaeoecology and palaeohydrology*, pp.703–713.
- Coope, G.R. 2001. Biostratigraphical distinction of interglacial coleopteran assemblages from southern Britain attributed to Oxygen Isotope Stages 5e and 7. *Quaternary Science Reviews* 20: 1717–1722.
- Darling, W.G., Bath, A.H., Talbot, J.C., 2003. The O & H stable isotopic composition of fresh waters in the British Isles. 2. Surface waters and groundwater. *Hydrology and Earth System Sciences* 7, 183–195.
- De Deckker, P., Chivas, A.R. & Shelley, J.M.G. 1999. Uptake of Mg and Sr in the euryhaline ostracod *Cyprideis* determined from in vitro experiments. *Palaeogeography Palaeoclimatology Palaeoecology*, 148, 105–116.
- Dettman, D.L. & Dwyer, G.S. 2012. The calibration of environmental controls on elemental ratios in ostracod shell calcite: a critical assessment. In: Horne, D.J., Holmes, J.A., Rodriguez-Lazaro, J. & Viehberg, F. (eds) *Ostracoda as Proxies for Quaternary Climate Change. Developments in Quaternary Science*, 17, 145–163.
- Devoy, R.J.N., 1979. Flandrian sea level changes and vegetational history of the lower Thames estuary. *Philosophical Transactions of the Royal Society B: Biological Sciences*, 285(1010), pp.355–407.
- Duller, G.A., 2008. Single-grain optical dating of Quaternary sediments: why aliquot size matters in luminescence dating. *Boreas*, 37(4), pp.589–612.
- Gibbard, P.L., 1994. *Pleistocene history of the Lower Thames valley*. Cambridge University Press.
- Green, C., Branch, N., Russell Coope, G., Schwenninger, J., Schreve, D., Field, M., Keen, D., Wells, J., Canti, M., Preece, R. & Gleed-Owen, C., 2006. Marine Isotope Stage 9 environments of fluvial deposits at Hackney, north London, UK. *Quaternary Science Reviews* 25, 89–113.
- Gibbard, P.L. and Preece, R.C. (1999) South and southeast England, In: Bowen, D.Q. (ed.), *A Revised correlation of Quaternary deposits in the British Isles*. Geological Society Special Report 23, 59–65, The Geological Society, Bath.
- Gupta, S., Collier, J.S., Garcia-Moreno, D., Oggioni, F., Trentesaux, A., Vanneste, K., De Batist, M., Camelbeeck, T., Potter, G., Van Vliet-Lanoë, B. and Arthur, J.C., 2017. Two-stage opening of the Dover Strait and the origin of island Britain. *Nature Communications*, 8.
- Hatch, M. 2014. The Pleistocene Solent River and its Major Tributaries: Reinterpreting the Fluvial Terrace Stratigraphy as a Framework for the Palaeolithic Archaeology of the Region. Unpublished PhD thesis, Queen Mary, University of London.

- Hatch, M., Davis, R.J., Lewis, S.G., Ashton, N., Briant, R.M. submitted. A revised Middle-Late Pleistocene terrace stratigraphy of the Western Solent (Christchurch Bay to Southampton Water): a framework for the Palaeolithic archaeology of the Solent region.
- Heip, C. 1976a. The life-cycle of *Cyprideis torosa* (Crustacea, Ostracoda). *Oecologia*, 24, 229–245.
- Heip, C. 1976b. The spatial pattern of *Cyprideis torosa* (Jones, 1850) (Crustacea:Ostracoda). *Journal of Marine Biological Association of the United Kingdom*, 56, 179–189.
- Holmes, J.A. and De Deckker, P., 2012. The Chemical Composition of Ostracod Shells. *Applications in Quaternary Palaeoclimatology*.
- Holmes, J.A. & De Deckker, P. 2015. Trace-element and stable-isotope composition of the *Cyprideis torosa* (Crustacea, Ostracoda) shell. *Journal of Micropalaeontology*, doi:10.1144/jmpaleo2015-024.
- Horne, D.J., 2007. A mutual temperature range method for Quaternary palaeoclimatic analysis using European nonmarine Ostracoda. *Quaternary Science Reviews*, 26(9-10), pp.1398-1415.
- Kaufman, D.S. and Manley, W.F., 1998. A new procedure for determining DL amino acid ratios in fossils using reverse phase liquid chromatography. *Quaternary Science Reviews*, 17(11), pp.987-1000.
- Keen, D.H. (1995) Raised beaches and sea-levels in the English Channel in the Middle and Late Pleistocene: problems of interpretation and implications for the isolation of the British Isles, in R.C.Preece (ed.), *Island Britain: a Quaternary perspective*, Geological Society of London Special Publication 96, 63-74, The Geological Society, Bath.
- Keen, D.H., Bateman, M.D., Coope, G.R., Field, M.H., Langford, H.E., Merry, J.S. and Mighall, T.M., 1999. Sedimentology, palaeoecology and geochronology of last interglacial deposits from Deeping St James, Lincolnshire, England. *Journal of Quaternary Science*, 14(5), pp.411-436.
- Kerney, M.P., 1999. *Atlas of the land and freshwater molluscs of Britain and Ireland*. Harley Books.
- Langford, H.E., Boreham, S., Briant, R.M., Coope, G.R., Horne, D.J., Penkman, K.E.H., Schreve, D.C., Whitehouse, N.J. and Whittaker, J.E., 2017. Evidence for the early onset of the Ipswichian thermal optimum: palaeoecology of Last Interglacial deposits at Whittlesey, eastern England. *Journal of the Geological Society*, 174(6), pp.988-1003.
- Leeder, M.R. and Stewart, M.D., 1996. Fluvial incision and sequence stratigraphy: alluvial responses to relative sea-level fall and their detection in the geological record. *Geological Society, London, Special Publications*, 103(1), pp.25-39.
- Lewis, S.G., Ashton, N. and Jacobi, R., 2011. Testing human presence during the Last Interglacial (MIS 5e): a review of the British evidence. In *Developments in Quaternary Sciences* (Vol. 14, pp. 125-164). Elsevier.
- Long, A.J., Scaife, R.G. and Edwards, R.J. 2000. Stratigraphic architecture, relative sea level and models of estuary development in southern England: New data from Southampton Water. In: Pye, K. and Allen, J.R.L. (eds.) *Coastal and estuary environments: sedimentology, geomorphology and geoarchaeology*. Geological Society Special Publication 175, p.253-280. Geological Society of London: London.

- Long, A.J., Barlow, N.L.M., Busschers, F.S., Cohen, K.M., Gehrels, W.R. and Wake, L.M., 2015. Near-field sea-level variability in northwest Europe and ice sheet stability during the last interglacial. *Quaternary Science Reviews*, 126, pp.26-40.
- Lucht W (1987) *Die Käfer Mitteleuropas*, Katalog. Goecke & Evers, Krefeld, pp 342
- Meisch, C., 2000. *Freshwater Ostracoda of western and central Europe (Vol. 8)*. Spektrum Akademischer Verlag.
- Mejdahl, V., 1979. Thermoluminescence dating: Beta-dose attenuation in quartz grains. *Archaeometry*, 21(1), pp.61-72.
- Murray, A.S. and Wintle, A.G., 2000. Luminescence dating of quartz using an improved single-aliquot regenerative-dose protocol. *Radiation measurements*, 32(1), pp.57-73.
- Parks, D.A. & Rendell, H.M. (1992) Thermoluminescence dating and geochemistry of loessic deposits in southeast England. *Journal of Quaternary Science* 7, 99-107.
- Peacock, J.D., 1993. Late Quaternary marine mollusca as palaeoenvironmental proxies: a compilation and assessment of basic numerical data for NE Atlantic species found in shallow water. *Quaternary Science Reviews*, 12(4), pp.263-275.
- Pedoja, Kevin, Julius Jara-Muñoz, Gino de Gelder, Jenni Robertson, Marco Meschis, David Fernández-Blanco, Maëlle NEXER, et al. 2017. "Neogene - Quaternary Slow Coastal Uplift of Western Europe Through the Perspective of Sequences of Strandlines from the Cotentin Peninsula (Normandy, France)". EarthArXiv. December 6. eartharxiv.org/5mt78.
- Penkman, K.E.H., Kaufman, D.S., Maddy, D. and Collins, M.J., 2008. Closed-system behaviour of the intra-crystalline fraction of amino acids in mollusc shells. *Quaternary Geochronology*, 3(1), pp.2-25.
- Penkman, K E H, Preece, R C, Bridgland, D R, Keen, D H, Meijer, T, Parfitt, S A, White, T S & Collins, M J, 2011, A chronological framework for the British Quaternary based on *Bithynia opercula*, *Nature*, **476**, 446-449.
- Phillips L. 1974. Vegetational history of the Ipswichian/Eemian Interglacial in Britain and continental Europe. *New Phytologist* 73: 589–604.
- Posamentier, H.W., Jervey, M.T. and Vail, P.R., 1988. Eustatic controls on clastic deposition I—conceptual framework.
- Posamentier, H.W. and Vail, P.R., 1988. Eustatic controls on clastic deposition II—sequence and systems tract models.
- Preece, R.C., Scourse, J.D., Houghton, S.D., Knudsen, K.L. and Penney, D.N. (1990) The Pleistocene sea-level and neotectonic history of the eastern Solent, southern England. *Philosophical Transactions of the Royal Society of London*, B 328, 425-477.
- Prescott, J.R. and Hutton, J.T., 1994. Cosmic ray contributions to dose rates for luminescence and ESR dating: large depths and long-term time variations. *Radiation measurements*, 23(2-3), pp.497-500.

- Reynolds, P.J. (1985) *The nature, origin and distribution of Quaternary brickearth and associated soils in south Hampshire*. Unpub. PhD thesis, University of London, 413pp.
- Reynolds, P.J. (1987) Lepe Cliff: the evidence for a pre-Devensian brickearth, in *Wessex and the Isle of Wight: Field Guide* (ed K.Barber), Quaternary Research Association, Cambridge, pp 21-22.
- Seaward, D.R., 1990. *Distribution of the marine molluscs of north west Europe*. Nature conservancy council.
- Schreve, D.C. (2001) Differentiation of the British late Middle Pleistocene interglacials: the evidence from mammalian biostratigraphy. *Quaternary Science Reviews* 20, 1693-1705.
- Shackleton, N.J., Berger, A. and Peltier, W.R., 1990. An alternative astronomical calibration of the lower Pleistocene timescale based on ODP Site 677. *Earth and environmental science transactions of the royal society of Edinburgh*, 81(4), pp.251-261.
- Siddall, M., Rohling, E.J., Almogi-Labin, A., Hemleben, C., Meischner, D., Schmelzer, I. and Smeed, D.A., 2003. Sea-level fluctuations during the last glacial cycle. *Nature*, 423(6942), pp.853-858.
- Sparks, B.W., 1964. Non-marine Mollusca and Quaternary ecology. *The Journal of Animal Ecology*, pp.87-98.
- Sutcliffe, A.J. 1995. Insularity of the British Isles 250,000 to 30,000 years ago: the mammalian, including human, evidence. In: *Island Britain: a Quaternary Perspective* (ed. R.C. Preece). Geological Society Special Publication No. 96, p. 127-140.
- Sykes, G.A., Collins, M.J. and Walton, D.I., 1995. The significance of a geochemically isolated intracrystalline organic fraction within biominerals. *Organic Geochemistry*, 23(11-12), pp.1059-1065.
- van der Meer, J.J.M., 1993. Microscopic evidence of subglacial deformation. *Quaternary Science Reviews*, 12, pp. 553-587.
- West, R.G. and Sparks, B.W. (1960) Coastal interglacial deposits of the English Channel. *Philosophical Transactions of the Royal Society of London*. B243, 95-133.
- Westaway, R.W.C., Bridgland, D.R. & White, M. 2006. The Quaternary uplift history of central southern England: evidence from the terraces of the Solent River system and nearby raised beaches. *Quaternary Science Reviews* 25: 2212–2250.

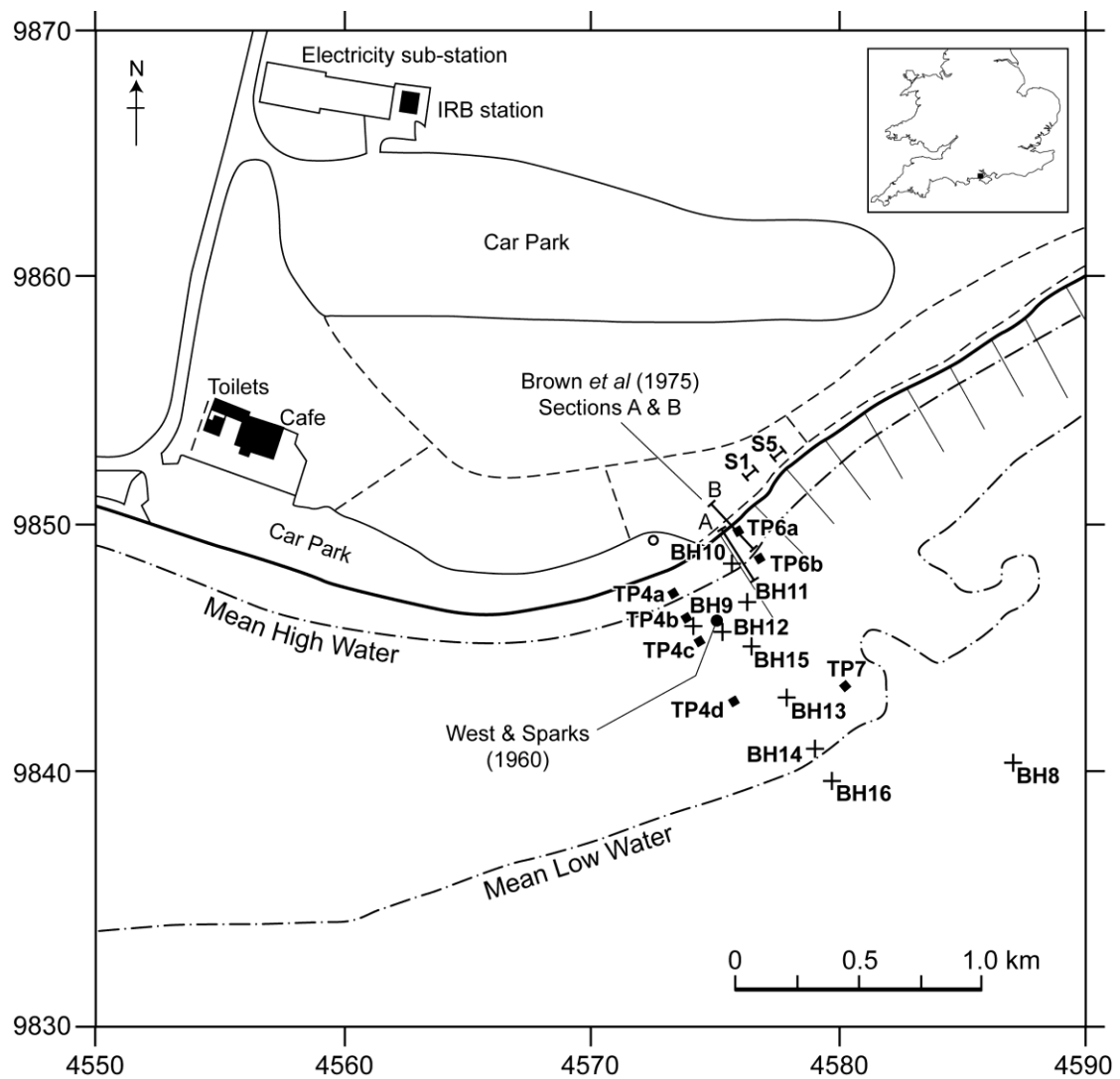


Figure 1. Maps showing the location of Lepe Country Park, Hampshire, England and sections, boreholes and test pits within it from all previous authors.

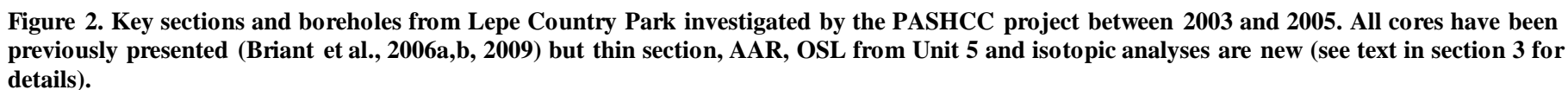


Figure 2. Key sections and boreholes from Lepe Country Park investigated by the PASHCC project between 2003 and 2005. All cores have been previously presented (Briant et al., 2006a,b, 2009) but thin section, AAR, OSL from Unit 5 and isotopic analyses are new (see text in section 3 for details).

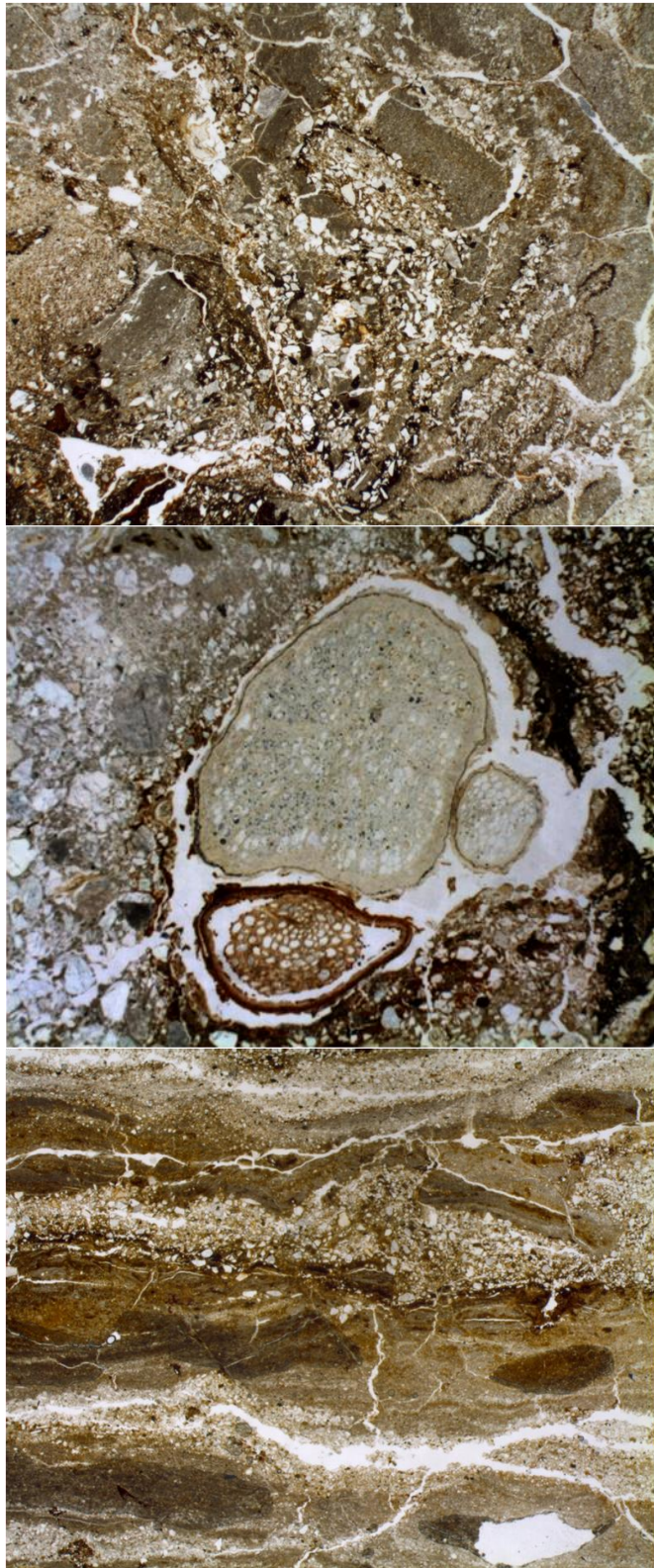


Figure 3. Photographs from thin sections from Unit 3 (63 x magnification); a) general view of LEPE03 KUB 1 (section 1); b) organic material in LEPE03 KUB 1 (section 1); c) LEPE03 monolith 6.5 (test pit 6b).

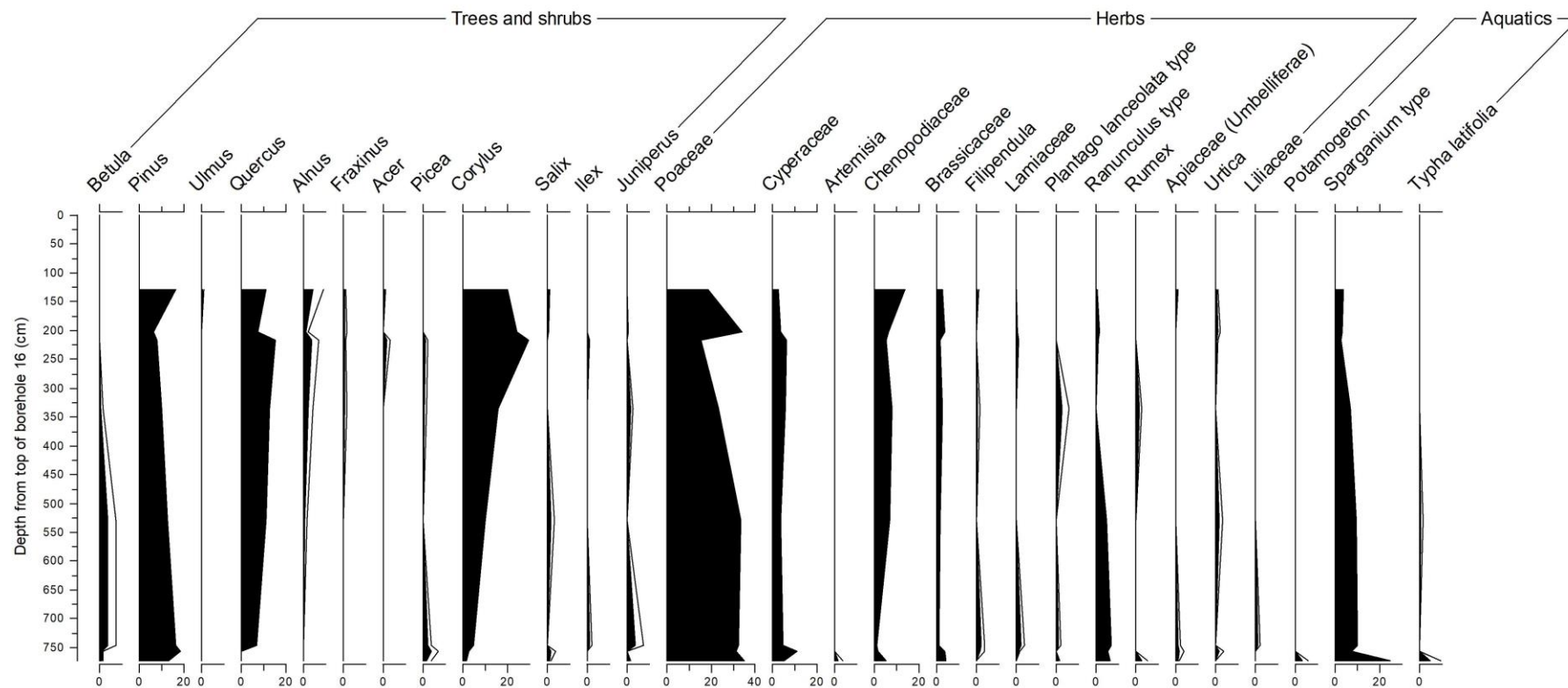


Figure 4. Pollen from Unit 2 in borehole 16. Main sum includes all terrestrial plants, including spores. Counts are low due to variable preservation.

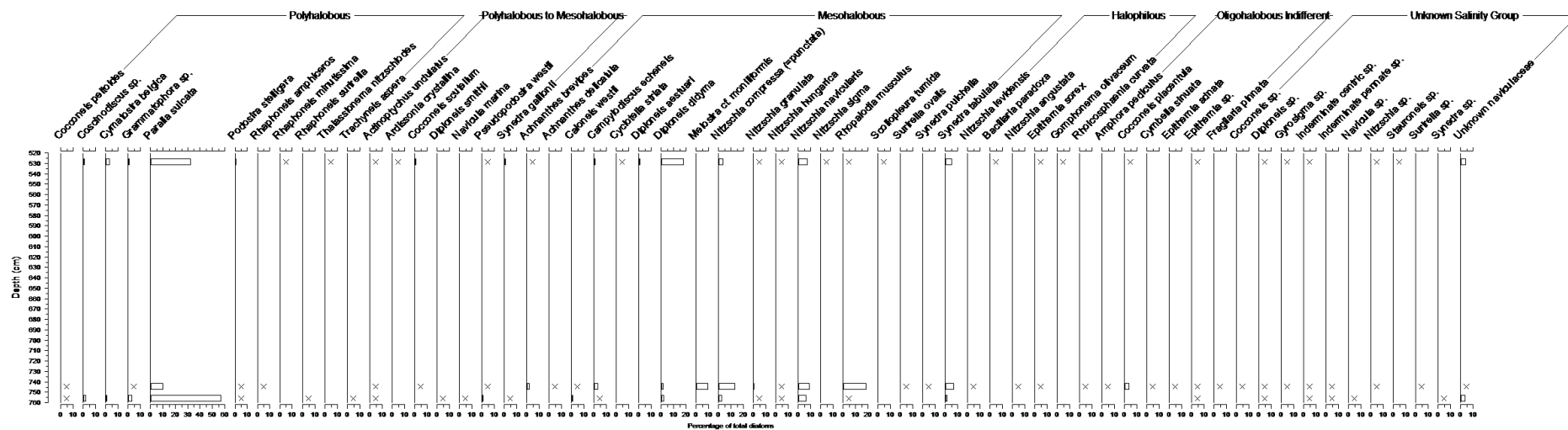


Figure 5. Diatom species abundances from Borehole 16.

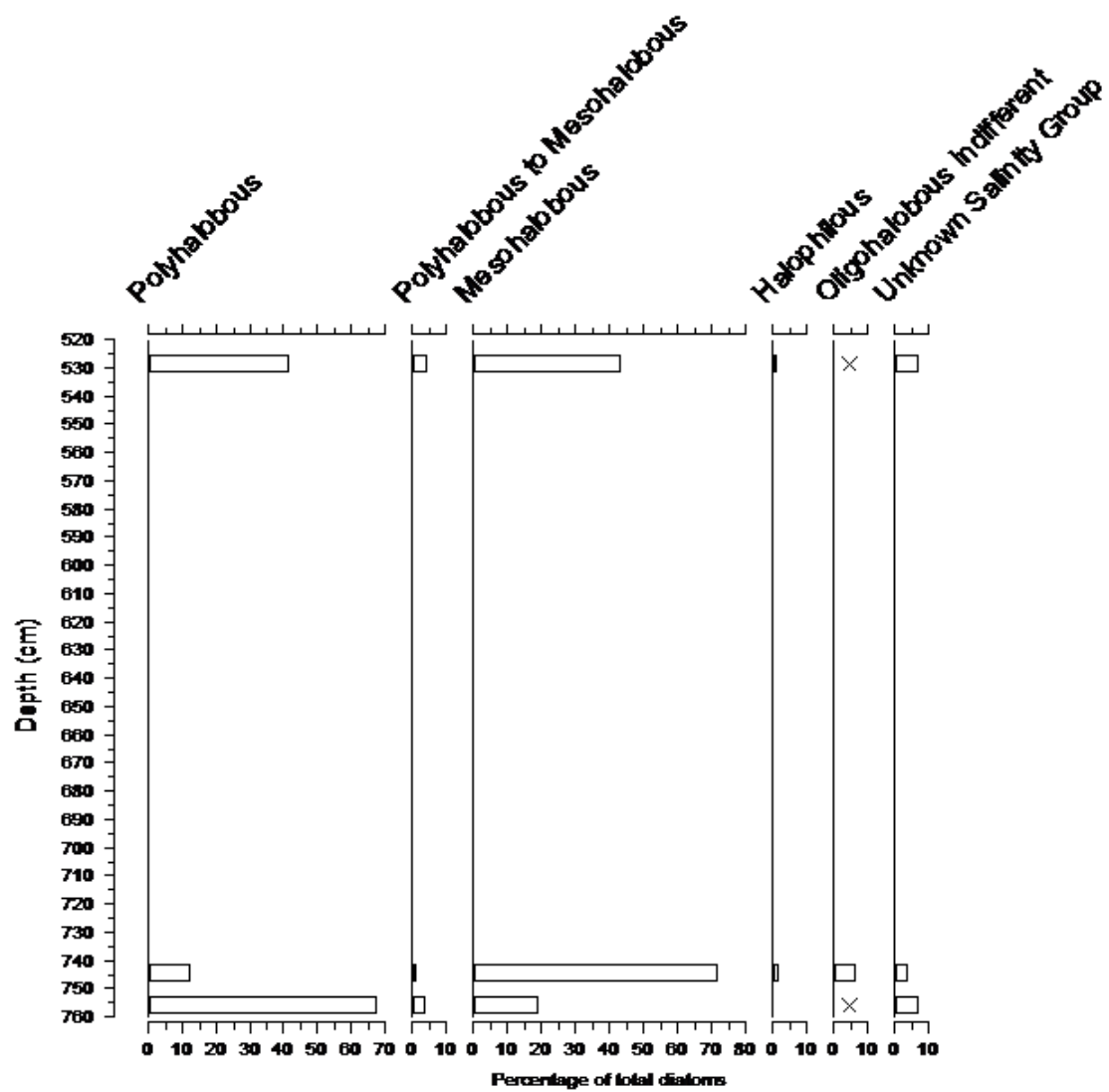


Figure 6. Abundances of diatoms in Borehole 16 by salinity group.

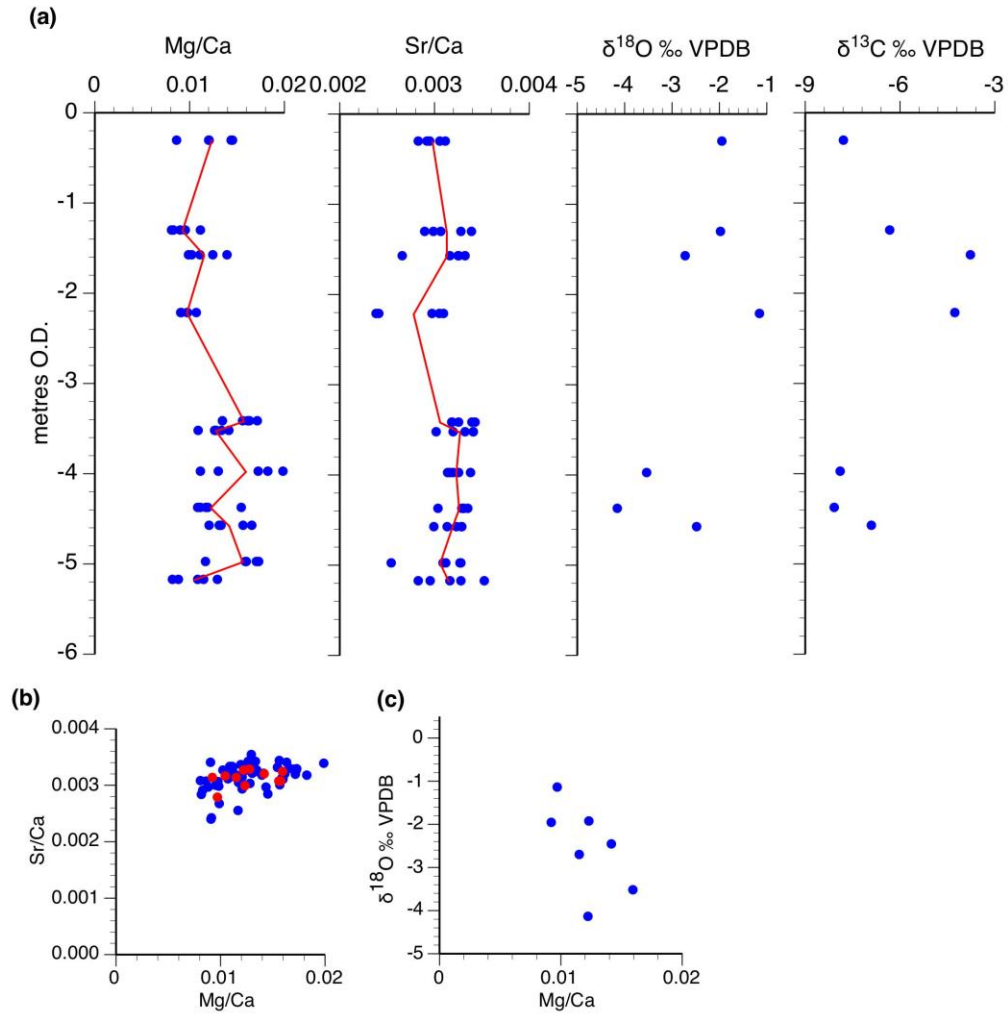


Figure 7. (a) Stratigraphic plot of Mg/Ca, Sr/Ca, $\delta^{18}\text{O}$ and $\delta^{13}\text{C}$ from the Stone Point sequence (b) Mg/Ca vs Sr/Ca (red = average values for each stratigraphic interval; blue = all data), (c) $\delta^{18}\text{O}$ vs Mg/Ca.

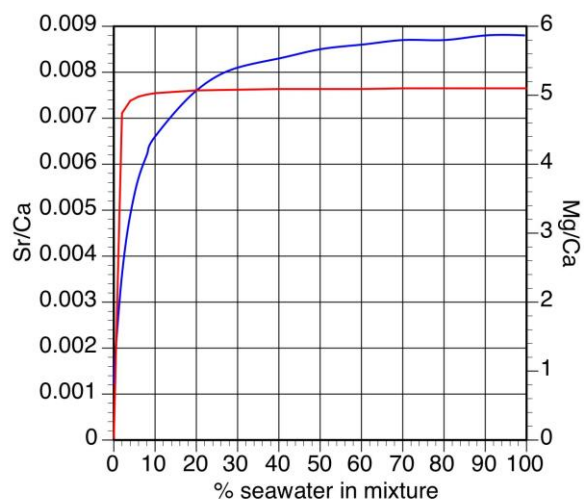


Figure 8. Mixing model to show change in Mg/Ca (red line) and Sr/Ca (blue line) of marginal-marine water with varying proportions of seawater in a seawater – meteoric water mixture. Seawater: [Mg] = 29.45 meqL⁻¹ and Mg/ Ca = 5.1; [Sr] = 0.1758 meqL⁻¹ and Sr/Ca = 0.0088) and chalk-derived groundwater: [Mg] = 0.028 meqL⁻¹ and Mg/ Ca = 5.1; [Sr] = 0.0079 meqL⁻¹ and Sr/Ca = 0.0012).

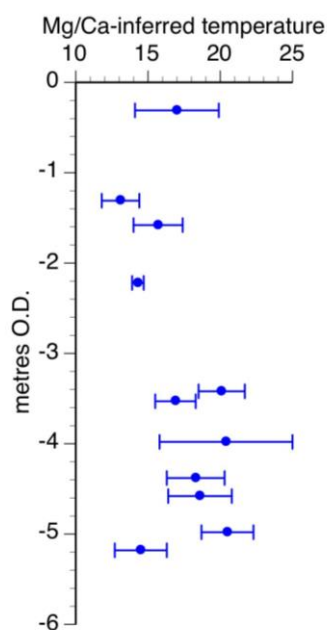


Figure 9. Reconstructed temperatures. Uncertainties are 1sd of the single shell; measurements at each level but do not attempt to include uncertainties in the Mg/Ca water estimates, which are an element in the palaeotemperature equation, nor of uncertainties in the equations itself. See text for further information.

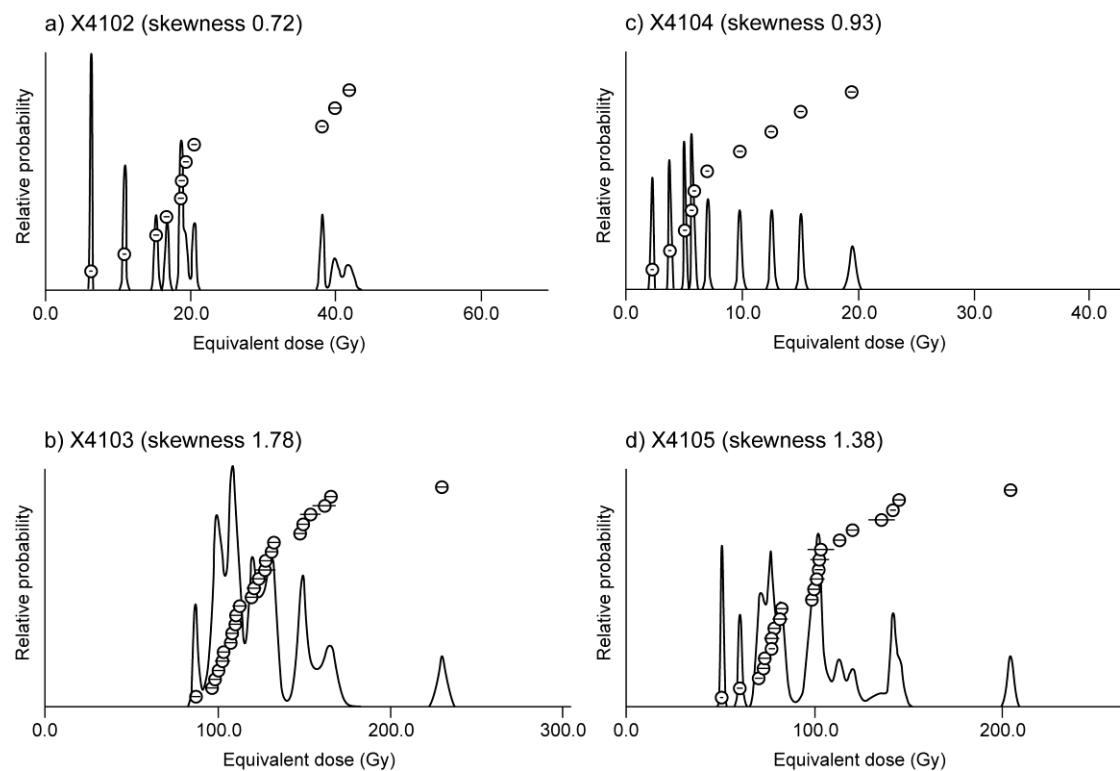


Figure 10. Equivalent dose (D_e) distributions for single aliquot measurements of samples a) LEP10-01 (X4102, 11 aliquots), b) LEP10-02 (X4103, 24 aliquots), c) LEP10-03 (X4104, 10 aliquots) and d) LEP10-04 (X4105, 22 aliquots). Skewness values for each are shown.

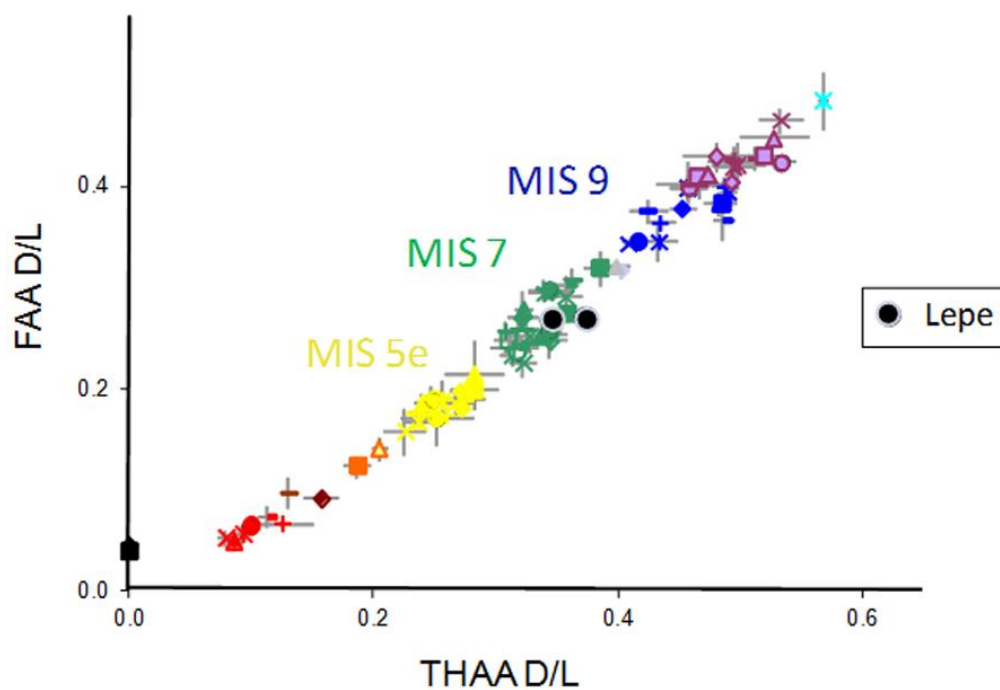


Figure 11. Free amino acid (FAA) vs Total (THAA) D/L values of Ala from bleached *Bithynia tentaculata* opercula from Lepe, compared with shells from UK sites (Penkman *et al.*, 2011) correlated with MIS 5e (yellow), MIS 7 (green) and MIS 9 (blue).

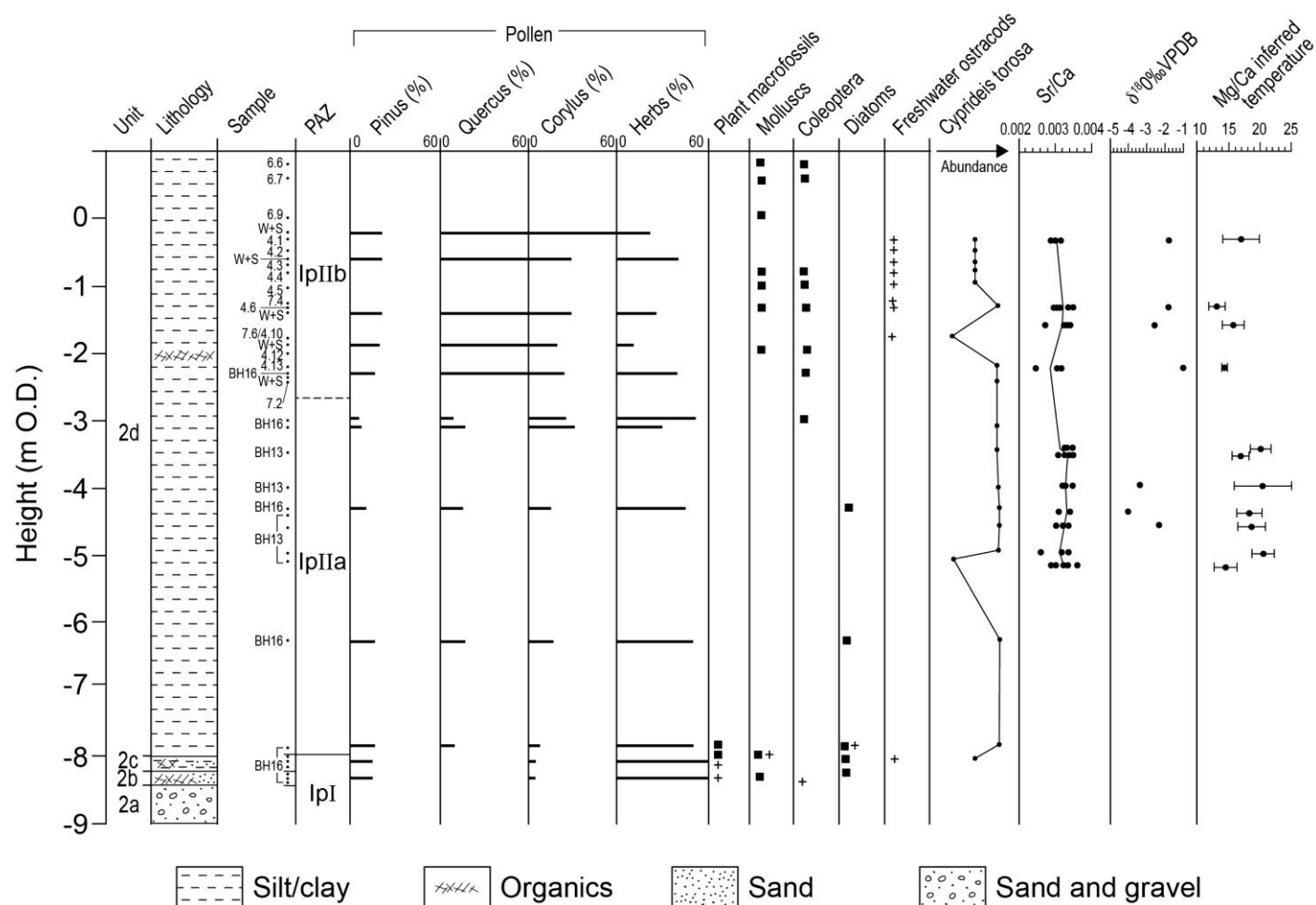


Figure 12. Summary of palaeoenvironmental and isotopic data from the Stone Point organic deposits. Data has been collated from West and Sparks (1960) – W+S, test pits 4a, 4b, 4d, 6a, 6b, 7 and boreholes 13 and 16. Filled squares denote brackish conditions and crosses freshwater conditions or presence of freshwater ostracods.

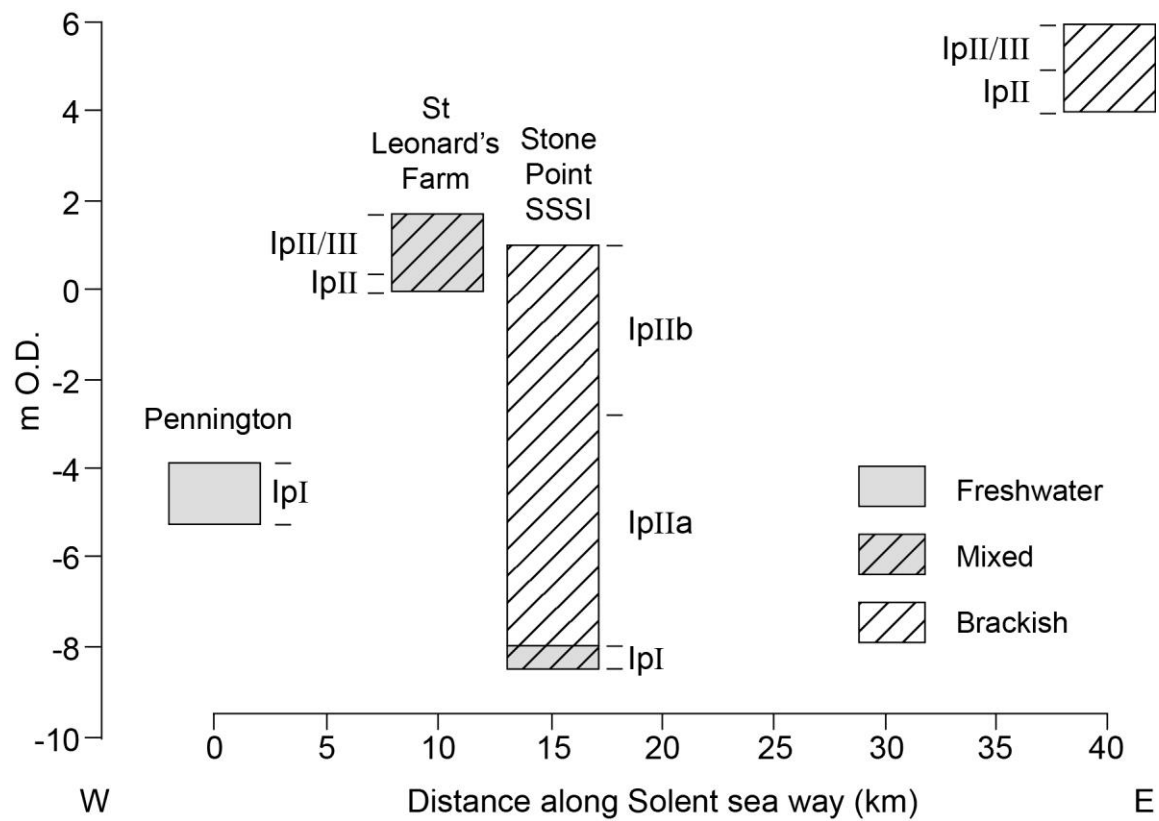


Figure 13. Comparison of key fossiliferous sequences along the Solent seaway: Pennington (Allen et al., 1996); St Leonard's Farm (Briant et al., 2013); Stone Point SSSI (this paper and references therein) and Bembridge Foreland (Preece et al., 1990).

	Reynolds (1985)				Parks (1990)			Section 1 (Briant et al, 2009)		
	Thickness (m)	Description	Particle size	Thin section features	Thickness (m)	Description	Particle size	Thickness (m)	Description	Particle size
'Upper brickearth'	Ah horizon 0.3 (0-0.3 m depth) Particle size sample 0.15-0.25 m depth	Dark greyish brown (10YR 4/2) very slightly stony sandy silt loam with fine gravel; roots and earthworm channels.	Modal size fraction 4-3 phi; 33% sand.	Yellowish brown (Holocene) clay illuviation, 75% as undisturbed argillans.	0.9 – 1.1 (c. 0.5-1.5 m depth - contacts irregular) LP1/2 at a depth of 1.1 m below ground surface	Reddish yellow (7.5 YR 6/6) medium silt / loess	Median particle size 25.5 microns	0.51 (0-0.51 m depth) LEP10-01,02 at 0.38 m depth below ground surface	Fine sand / silt, becoming slightly clayey below c. 35 cm; occasional wasp/bee burrow and roots; occasional flint clasts; pale yellow (2.5 Y 7/4).	LEP10-01/X4102: modal size fraction 125-175 microns / 2.5-3 phi; median particle size 120 microns / 3 phi LEP10-02/X4103: modal size fraction 88-125 microns / 3-3.5 phi; median particle size 67 microns / 3.9 phi
	Eb horizon 0.18 (0.3-0.48 m depth)	Dark yellowish brown (10 YR 4/4) very slightly stony sandy silt loam; roots and earthworm channels.	-	-						
	Bt horizon 0.3 (0.48-0.78 m depth) Particle size sample 0.5-0.68 m depth Thin section sample 0.63-0.75 m depth	Strong brown (7.5 YR 4/6) very slightly stony clay loam; roots.	Modal size fraction 4-3 phi; 45% sand.	-						
'Lower brickearth'	2Bt horizon 0.4 (0.78-1.18 m depth) Particle size sample 0.8-0.9 m depth Thin section sample 1-1.08 m depth	Strong brown (7.5 YR 5/8) with yellowish brown (10YR 5/6) very slightly stony silty clay with very rare dark red (2.5 YR 3/6) mottles. Few roots and earthworm channels. Thin irregular stone lines of fine to medium gravel at 0.78 and 0.96 m depth.	Bimodal – main peak at 7-6 phi (silt fraction), secondary at 2-1 phi (sand). Total silt 90.3%; sand 9.7%.	74% egg-yellow illuvial clay, of which only 57% is undisturbed. 26% yellowish-brown illuvial clay (Holocene), of which 90% is undisturbed.	0.6 – 0.8 (c. 1.5-2.2 m depth - contacts irregular) LP3/4 at a depth of 1.75 m below ground surface	Reddish yellow (7.5 YR 6/8) medium silt / loess	Median particle size 7.5 microns	0.45 (0.51-0.96 m depth) LEP10-03,04 at 0.76 m depth below ground surface	As above, but yellowish red (5YR 5/8).	LEP10-03/X4104: modal size fraction 31-44 microns / 4.5-5 phi; median particle size 31 microns / 5 phi LEP10-04/X4105: modal size fraction 31-44 microns / 4.5-5 phi; median particle size 30 microns / 5 phi

Table 1. Summary of descriptions of Unit 5 at Stone Point SSSI from various studies. Note that in Briant et al. (2009), descriptions are simply of two overlying units – it was not clear which were equivalent to the previously defined upper and lower brickearths, although the Munsell colours described are similar for the lower unit only.

Taxon	Plant part	Sample (depth cm, Borehole 16)			
		740 - 746	750 - 755	761 - 768	772 - 777
		100 ml	100 ml	50 ml	50 ml
<i>Woodland & shade tolerant</i>					
<i>Alnus glutinosa</i>	fruit	-	1	2	1
<i>Betula</i> sp.	fruit (without wings)	-	-	-	1
<i>Cenococcum geophilum</i>	sclerotium	-	-	present	-
<i>Rubus idaeus</i>	seed	3	-	-	-
<i>Waterside & damp ground</i>					
Alismataceae sp.	fruit	-	-	-	1
<i>Bidens</i> sp.	barbed spine	-	-	-	1
<i>Eleocharis</i> cf. <i>palustris</i>	nutlet	-	-	-	3
<i>Epilobium</i> cf. <i>hirsutum</i>	seed	-	-	1	-
<i>Hypericum tetrapterum</i>	seed	-	1	-	-
<i>Lycopus europaeus</i>	nutlet	-	-	1	-
<i>Ranunculus</i> subgenus <i>Ranunculus</i> sp(p).	achene	-	-	1	5
<i>Scirpus maritimus</i>	nutlet	4	14	-	-
<i>Scirpus</i> sp(p).	nutlet	-	7	-	-
<i>Sparganium erectum</i>	fruitstone	-	-	3	1
<i>Typha</i> sp(p).	fruit	8	30	390	335
<i>Aquatic</i>					
Characeae sp(p).	oospore	2	2	12	8
<i>Hydrocharis morsus-ranae</i>	seed	-	-	1	2
<i>Potamogeton</i> sp.	fruit	1	-	-	-
<i>Ruppia</i> sp.	fruit	-	1	-	-
<i>Ruppia</i> sp.	fruit	-	1	-	-
<i>Zannichellia palustris</i>	fruit	-	1	-	-
<i>Unclassified</i>					
<i>Carex</i> sp(p).	biconvex nutlet	-	-	4	2
<i>Carex</i> sp(p).	trigonus nutlet	-	-	2	-
<i>Carex</i> sp(p).	nutlet and utricle	-	-	5	-
<i>Juncus</i> sp(p).	seed	-	6	33	63
Laminaceae sp.	nutlet	-	-	1	-
<i>Mentha</i> cf. <i>aquatica</i>	nutlet	-	-	2	2
<i>Urtica dioica</i>	achene	-	-	-	3
<i>Undetermined taxon</i>	budscales	-	-	1	-
Total number of remains (excluding oospores)		18	64	458	428
Total number of taxa		5	9	13	14

Table 2. Plant macrofossil analysis from samples from Borehole 16.

	TP4d	TP4b			TP6a		
Sample	4.12	4.4	4.5	4.6	6.6	6.7	6.9
<i>Hydrobia ventrosa</i> (Montagu, 1803)	7	2	1	128			
<i>Hydrobia ulvae</i> (Pennant, 1777)	1			39			
<i>Hydrobia</i> spp.	45	30	10	1132			1
<i>Ovatella myosotis</i> (Draparnaud, 1801)		2	1	17			
<i>Cerastoderma edule</i> (Linné, 1758)		2		1			
<i>Scrobicularia plana</i> (da Costa, 1778)		11	4	35			
<i>Abra</i> spp.		1		4			
<i>Total</i> (6 species)	53	48	16	1356	0	0	1

Table 3. Molluscs from the upper part of Unit 2d (test pits 4b, 4d and 6a)

	Unit 2d											Unit 2b
		TP7	TP6b	TP6a			TP4d	TP4b			BH16	BH16
	1974 sample	7.5	6.10	6.8	6.7	6.6	4.12	4.6	4.5	4.4	125 – 127 cm 200 cm	774 – 779 cm
Carabidae												
<i>Elaphrus riparius</i> (L.)		1										
<i>Dyschirius salinus</i> Schaum	1		2		3					1		
<i>Dyschirius aeneus</i> (Dej.)	1		1	1	1				1	1		
<i>Paratachys bistriatus</i> (Duft.)			1					2		1		
* <i>Porotachys bisulcatus</i> (Nicol.)									2	1		
<i>Bembidion obliquum</i> Sturm	1	3	1						1	1		
<i>Bembidion varium</i> (Ol.)	1		2	1	3	1	2	2	2	2	1	
<i>Bembidion nitidulum</i> (Marsh.)									1	1		
* <i>Bembidion elongatum</i> Dej.	1											
<i>Bembidion assimile</i> Gyll.	5	2	1	1	2	1	2	2	2	2		
<i>Bembidion fumigatum</i> (Duft.)									1			
<i>Bembidion normanum</i> Dej.			2		1		1	1	2	2	1	1
<i>Bembidion minimum</i> (F.)	1	1	2	1	2	1	1		1	2		
<i>Bembidion articulatum</i> (Panz.)		1	1						2			
<i>Bembidion octomaculatum</i> (Goeze)						1			1			
<i>Bembidion iricolor</i> Bedel,									1			
<i>Bembidion guttula</i> (F.)			1									
<i>Pogonus litoralis</i> (Duft.)	1				1		1	1	1			
<i>Acupalpus</i> sp.					1							
<i>Poecilus</i> sp.	1								1			
<i>Pterostichus vernalis</i> (Panz.)	2							1		1		
<i>Pterostichus nigrita</i> (Payk.)	1		1									
<i>Pterostichus minor</i> (Gyll.)		1								1		
<i>Pterostichus atterimus</i> (Hbst.)			1						1			
<i>Agonum muelleri</i> (Hbst.)	1									1		
<i>Agonum thoreyi</i> Dej.	1	1	2									
<i>Amara convexiuscula</i> (Marsh.)	1											
<i>Chlaenius tristis</i> (Schall.)		1					1			1		
<i>Oodes helopioides</i> (F.)								1				
* <i>Oodes gracilis</i> Villa	2	2	1				1	3	1	1		
<i>Odacantha melanura</i> (L.)	3	14	5	2	1	1	5	1	1	2		
<i>Demetrias monostigma</i> Sam.		2										
<i>Demetrias imperialis</i> (Germ.)		2		1								
<i>Paradromius longiceps</i> Dej.							4	1	1	1		
Haliplidae												
<i>Peltodytes caesus</i> (Duft.)								1	1			
Dytiscidae												
* <i>Hydroglyphus pusillus</i> (F.)	1	1				2		1	2	3		
<i>Hydrovatus cuspidatus</i> (Kunze)	2	16		1			2	3	6	13		
<i>Coelambus impressopunctatus</i> (Schall.)		1										
<i>Coelambus parallelogrammus</i> (Abr.)		1								1		
<i>Hygrotus inaequalis</i> (F.)		1	1				2			1		
<i>Hydroporus</i> spp.		2	2			1	5	1	1	1	1	
<i>Graptodytes bilineatus</i> (Sturm)										1		
<i>Noterus clavicornis</i> (Geer)	1	6	1			1	1	1	2	2	1	

<i>Noterus crassicornis</i> (Müll.)		2						2				
<i>Agabus bipustulatus</i> (L.)							1					
<i>Agabus</i> sp.		1					1	1				
<i>Ilybius</i> sp.							1					
<i>Rhantus</i> sp.	1						1	1				
<i>Colymbetes fuscus</i> (L.)	1	1					1	1	1			
<i>Graphoderus</i> sp.	1	1					1	1	1			
<i>*Cybister lateralmarginalis</i> (Geer)									1			
Gyrinidae												
<i>Gyrinus caspius</i> Mènètr.	1	5	1	1		1	1	5	2	5		
Hydraenidae												
<i>Hydraena gracilis</i> Germ.				1								
<i>Hydraena cf riparia</i> Kug.							1					
<i>Ochthebius dilatatus</i> Steph.							1					
<i>Ochthebius minimus</i> (F.)	4	1	1	1		1		2	1			
<i>*Ochthebius foveolatus</i> Germ.	1											
<i>Ochthebius marinus</i> (Payk.)			1		5		1	1				
<i>Ochthebius viridis</i> Peyrhff. / <i>pusillus</i> Steph.	1	1					1	1	2			
<i>Ochthebius</i> sp.	6	18	10	1	4	1	3	3	10	14	1	1
<i>Limnebius aluta</i> Bedel	2	2	5			1		5		1	1	
<i>Hydrochus carinatus</i> Germ.										1		
<i>Helophorus</i> misc.small spp.	1		1		1	1		1	1	1		
Hydrophilidae												
<i>Coelostoma orbiculare</i> (F.)	2	3	2	1	2		3	2	4	8		
<i>Sphaeridium scarabaeoides</i> (L.) / <i>lunatum</i> F.												1
<i>Sphaeridium</i> sp.	1							1	1			
<i>Cercyon ustulatus</i> (Preysl.)								1	1			
<i>Cercyon melanocephalus</i> (L.)								1				
<i>Cercyon marinus</i> Thoms.									1			
<i>Cercyon pygmaeus</i> (Illiger)								1				
<i>Cercyon tristis</i> (Illiger)		1									1	
<i>Cercyon convexiusculus</i> Steph.	1	1					2	1	1	3		
<i>Cercyon sternalis</i> Shp.	4	5	3	3				5	11	6		
<i>Cercyon analis</i> (Payk.)	1	1	1	2	3			1		3		
<i>Cercyon</i> sp.												1
<i>Megasternum obscurum</i> (Marsh.)												1
<i>Paracymus aeneus</i> (Germ.)	7	28	21	11	17	8	36	17	27	28	2	2
<i>Hydrobius fuscipes</i> (L.)	1	1	1					1	1	1		
<i>Limnoxenus niger</i> (Zschach)	1	2	1		1		1	1	2	1		1
<i>Laccobius</i> sp.	1	1	1			1						
<i>Helochares</i> sp								1				
<i>Enochrus affinis</i> (Thunb.)											1	
<i>Enochrus</i> sp.	8	34	17	2	5	4	10	15	15	25		2
<i>Cymbiodyta marginella</i> (F.)	3	7	1	1	2	2	1		2	3		
<i>Hydrochara caraboides</i> (L.)						1		1	1			
<i>Hydrophilus piceus</i> (L.)									1	1		
<i>Berosus luridus</i> (L.)		1			1	1		1	2	1		
Histeridae												
<i>Acritus homoeopathicus</i> Woll.				1			1					
<i>Hister (sensu lato)</i> sp.		1		1				1	1			
Silphidae												
<i>Phosphuga atrata</i> (L.)			1									
Opthoperidae												
<i>Corylophus crassidoides</i> (Marsh.)	6	2	2	1	2	3	1	1	1	1		

[illegible]

* <i>Airaphilus elongatus</i> (Gyll.)					1	1	1		1				
Heteroceridae													
<i>Heterocerus</i> sp.			4			2		1	2	3	4		
Byrrhidae													
* <i>Pelochares versicolor</i> (Waltl)									1				
<i>Byrrhus</i> sp.											1		
Nitidulidae													
<i>Meligethes</i> sp.			1								1		
<i>Epuria</i> sp.			1	1		1	1		1	1			
Phalacridae													
<i>Stilbus oblongus</i> (Er.)		2	25	6	3	8	3	3	5	10	9		1
Lathridiidae													
<i>Corticarina</i> sp.			3	1	1				1	2	4		
Mycetophagidae													
* <i>Berginus tamariski</i> Woll.						1							
Coccinellidae													
<i>Coccidula rufa</i> (Hbst.)											1		
<i>Anisosticta novemdecimpunctata</i> (L.)						1							
<i>Coccinella undecimpunctata</i> L.								1	1			1	1
Bostrichidae													
<i>Bostrychus capucinus</i> (L.)									1				
Anobiidae													
<i>Anobium</i> sp.		1							1				
Anthicidae													
<i>Anthicus antherinus</i> (L.)				1									
* <i>Cordicomus gracilis</i> (Panz.)			2	1				1					
<i>Cordicomus</i> sp.		1	4		2	1		1	1	2	2		1
Tenebrionidae													
<i>Opatrum sabulosum</i> (L.)									1				
<i>Eledona agaricola</i> (Hbst.)							1						
Scarabaeidae													
* <i>Euoniticellus fulvus</i> (Goeze)							1						
<i>Copris lunaris</i> (L.)									1				
* <i>Caccobius schreberi</i> (L.)		1	1								1		
* <i>Onthophagus massai</i> Barraud		1	2	1	1	1	?	?	1	2	2		
<i>Onthophagus verticornis</i> (Laich.)											1		
<i>Onthophagus fracticornis</i> (Preysl.)										1			
* <i>Aphodius cf carpetanus</i> Graëlls		1				1			1				
<i>Aphodius sticticus</i> (Panz.)			1										
* <i>Aphodius</i> sp.										1			
<i>Aphodius</i> sp.		2	1	2	2	2	3		3	3	1		
* <i>Heptaulacus</i> sp.				1									
<i>Melolontha melolontha</i> (L.)											1		
<i>Cetonia aurata</i> (L.)		1							1		1		
Lucanidae													
<i>Lucanus cervus</i> (L.)									1				
<i>Dorcus parallelipedus</i> (L.)					1						1		

Chrysomelidae																	
<i>Donacia clavipes</i> F.								1									
<i>Donacia thalassina</i> Germ.	12	27	11	1	9	2	3	3	2	5							
<i>Donacia cinerea</i> Hbst.		2	1	1				1	1	1						1	
<i>Donacia</i> sp.											1	1				1	
<i>Plateumaris sericea</i> (L.)		1					1									1	
<i>Plateumaris braccata</i> (Scop.)	4	4	4	2	3	7	2	1	3	4		1				1	
<i>Haltica</i> sp.								1	2	1							
<i>Chaetocnema cf concinna</i> (Marsh.)		1			3				1	2							
<i>Chaetocnema</i> sp.		1															
<i>Psylliodes</i> sp.	1								2								
Bruchidae																	
<i>Bruchus</i> sp / <i>Bruchidius</i> sp.			1		1			1									
Scolytidae																	
* <i>Scolytus carpini</i> (Ratz.)					2	1											
<i>Hylastes angustatus</i> (Hbst.)		1															
<i>Hylurgops palliatus</i> (Gyll.)				1													
<i>Hylesinus crenatus</i> (F.)										1							
<i>Hylesinus oleiperda</i> (F.)		1															
Platypodidae																	
<i>Platypus cylindrus</i> (F.)									1								
Curculionidae																	
<i>Apion</i> sp.			2	1					2	1							
<i>Phloeophagus lignarius</i> (Marsh.)								1		1							
<i>Phloeophagus cf gracilis</i> Rosh.					1												
* <i>Brachytemnus porcatus</i> (Germ.)					1												
<i>Bagous</i> sp.	1				4		1	1	1	1							
<i>Tanysphyrus lemnae</i> (Payk.)	5	1	27	1	1			1	1	1							
<i>Notaris scirpi</i> (F.)									1								
<i>Thryogenes neries</i> (Payk.) / <i>festucae</i> (Hbst.)																1	
<i>Thryogenes</i> sp.	5	9	6	2	4	1	4		7	4							
* <i>Bradybatus</i> sp						1											
<i>Curculio venosus</i> (Grav.)			1	1	1	1		1	1	1							
<i>Curculio nucum</i> L.			1														
<i>Hylobius abietis</i> (L.)									1								
* <i>Camptorhynchus simplex</i> Seidl.									1								
<i>Ceutorhynchus</i> sp.			1				1										
<i>Rhynchaenus quercus</i> (L.)	1	1	2	2			1	6	2	3							
<i>Rhynchaenus</i> sp							1		1								

Table 4. Coleoptera from various parts of Units 2b and 2d.

			FORAMINIFERA							OSTRACODA						
			<i>Ammonia aberdoveyensis</i>	<i>Ammonia limnetes</i>	<i>Elphidium waddense</i>	<i>Elphidium williamsoni</i>	<i>Haynesina germanica</i>	<i>Quinqueloculina</i> sp. (brown)	<i>Trochammina inflata</i>	Freshwater ostracods	<i>Cyprideis torosa</i>	<i>Loxoconcha elliptica</i>	<i>Leptocythere porcellanea</i>	<i>Leptocythere castanea</i>	<i>Cytherois</i> sp.	<i>Elofsonia baltica</i>
2d	TP 4b	4.1*	x	x	x					o	xx					
		4.2	x	x	x					x	xx	x	x			
		4.3	x	x	x			o		x	xx	x	x			
		4.4	x	x	x		x			x	xx	x				
		4.5	xx	xx	x	x	x			x	xx					
		4.6*	xx	x	xx	x	x			x	xxx	x				
	TP 4d	4.8	x	xx	x	o	x				x		x			
		4.9	x	x			x				x		x			
		4.10	x	x	x		x			o	x	x	xx			
		4.11	x	x	x		x				x	x	x			
		4.13*	xxx	xx	x	x	x				xxx	x				
		4.14	xx		x	x	x				x					
	TP 7	7.1														
		7.2	xx	xx			x									
		7.3	xx	xx			x									
		7.4	x	x	x				x	x						
		7.5														
		7.6*	xx	x	x				x		x					
		7.7	x	xx	x						x					
		7.8	xxx	xx	xx	xx	xx				x		xx			
		7.9	xx	xx	x	xx	x	xx								
		7.10	xx	xx	xx	x	x	x			x		x			
		7.11	xx	x	xx	x	x				x		x	o		
		7.12*	x	xx	x						xxx		xx	xx		
	BH 13	320 cm*	xx		x		x				xxx	xx	x	x		
		345 cm	xxx		x		x				xxx	xx	xx	xx	x	
		365 cm*	xxx		xx		x				xxxx	xx	x	x		
		385 cm	xx		xx		x				xxx	x	xx	x		
		405 cm*	xx		xx		o				xxxx	x	xx			
		425 cm*	xx		x		x				xxxx	xx	x			o
		445 cm	xx		x		x				xxx	x	xx			o
		465 cm*	xx		x						xxx	x	x			
		475 cm	xx		x						xxx	x	x			
		485 cm*	x		x						xx	o				
		491 cm	x								x		x			
		497 cm														
	BH16	127 cm														
		201 cm	x	x	x		x									
		218 cm	xxx	xxx	xxx						xxx					
		336 cm	xxx		xx		x				xxx	xxx	x	x		
		530 cm	xxx		xx		x				xxx	xx	x			
		747 cm	xxx		xxx						xxx	xx	x			
2c		758 cm	xx		x					x	xx	x	x			
2b		773 cm														

Table 5. Ostracoda and foraminifera from Units 2b to 2d. o - one specimen; x - present (several specimens); xx - common; xxx – abundant. Starred samples are those from which isotope measurements are reported in Table S6.

Section/borehole	Level	HEIGHT m OD	Mg/Ca C. torosa	Sr/Ca C. torosa	Mg/Ca average	Mg/Ca 1sd	Sr/Ca average	Sr/Ca 1sd	d ¹³ C C. torosa	d ¹⁸ O C. torosa	Sr/Ca water (Kd[Sr]=0.47 Kd[Sr]=0.47	Sr/Ca (water) average	Sr/Ca (water) 1sd	Inferred temperature		Inferred temperature	
														Mg/Ca _(water) calculated from Sr/Ca	T °C	average T °C	1sd
Lepe Borehole 13	480/490cm	-5.18	0.01089	0.00328							0.00698			4.7	14.7		
		-5.18	0.00820	0.00283							0.00602			4.4	12.4		
		-5.18	0.01151	0.00317							0.00674			4.7	15.6		
		-5.18	0.00883	0.00295							0.00629			4.5	12.9		
		-5.18	0.01296	0.00353	0.01048	0.00195	0.00315	0.00027			0.00751	0.00671	0.00058	4.8	16.7		
Lepe Borehole 13	460/470cm	-4.98	0.01732	0.00328							0.00698			4.7	21.9		
		-4.98	0.01599	0.00309							0.00658			4.6	20.8		
		-4.98	0.01705	0.00327							0.00696			4.7	21.6		
		-4.98	0.01593	0.00312							0.00664			4.6	20.7		
		-4.98	0.01170	0.00255	0.01560	0.00227	0.00306	0.00030			0.00542	0.00651	0.00064	4.2	17.3	20.5	1.8
Lepe Borehole 13	420/430cm	-4.58	0.01659	0.00329							0.00700			4.7	21.0		
		-4.58	0.01315	0.00329							0.00699			4.7	17.2		
		-4.58	0.01211	0.00313							0.00667			4.6	16.3		
		-4.58	0.01569	0.00300							0.00638			4.5	20.7		
		-4.58	0.01336	0.00323	0.01418	0.00188	0.00319	0.00012	-6.90	-2.47	0.00688	0.00678	0.00026	4.7	17.6	18.6	2.2
Lepe Borehole 13	400/410cm	-4.38	0.01118	0.00331							0.00705			4.7	15.0		
		-4.38	0.01548	0.00331							0.00704			4.7	19.8		
		-4.38	0.01174	0.00304							0.00646			4.6	16.1		
		-4.38	0.01195	0.00335							0.00713			4.8	15.8		
		-4.38	0.01085	0.00329	0.01224	0.00187	0.00326	0.00013	-8.07	-4.15	0.00700	0.00694	0.00027	4.7	14.7	18.3	2.0
Lepe Borehole 13	360/370cm	-3.98	0.01829	0.00317							0.00673			4.7	23.2		
		-3.98	0.01989	0.00338							0.00719			4.8	24.5		
		-3.98	0.01307	0.00320							0.00680			4.7	17.3		
		-3.98	0.01115	0.00314							0.00668			4.6	15.3		
		-3.98	0.01727	0.00326	0.01594	0.00368	0.00323	0.00010	-7.89	-3.53	0.00693	0.00687	0.00020	4.7	21.9	20.4	4.6
Lepe Borehole 13	315/325cm	-3.53	0.01091	0.00332							0.00707			4.7	14.7		
		-3.53	0.01282	0.00302							0.00643			4.6	17.4		
		-3.53	0.01338	0.00341							0.00726			4.8	17.3		
		-3.53	0.01268	0.00341							0.00726			4.8	16.5		
		-3.53	0.01416	0.00320	0.01279	0.00120	0.00327	0.00017			0.00681	0.00696	0.00035	4.7	18.5	16.9	1.4
Lepe Trench 7	7.12	-3.42	0.01350	0.00325							0.00692			4.7	17.7		
		-3.42	0.01717	0.00318							0.00677			4.7	21.9		
		-3.42	0.01563	0.00343							0.00730			4.8	19.7		
		-3.42	0.01617	0.00319							0.00679			4.7	20.8		
		-3.42	0.01635	0.00340	0.01576	0.00138	0.00330	0.00010			0.00723	0.00700	0.00025	4.8	20.6	20.1	1.6
Lepe Trench 7	7.6	-2.22	0.00909	0.00239							0.00508			4.0	14.5		
		-2.22	0.00978	0.00305							0.00650			4.6	13.8		
		-2.22	0.00983	0.00298							0.00633			4.5	14.0		
		-2.22	0.00915	0.00241							0.00513			4.1	14.5		

		-2.22	0.01075	0.00310	0.00972	0.00067	0.00278	0.00036	-4.26	-1.15	0.00659	0.00593	0.00076	4.6	14.9	14.3	0.4
Lepe Trench 4	4.13	-1.58	0.01111	0.00332							0.00707			4.7	14.9		
		-1.58	0.00989	0.00266							0.00566			4.3	14.8		
		-1.58	0.01025	0.00325							0.00693			4.7	14.1		
		-1.58	0.01249	0.00325							0.00692			4.7	16.6		
		-1.58	0.01397	0.00317	0.01154	0.00169	0.00313	0.00027	-3.76	-2.72	0.00674	0.00666	0.00057	4.7	18.4	15.7	1.7
Lepe Trench 4	4.6	-1.31	0.00811	0.00307							0.00653			4.6	11.9		
		-1.31	0.01117	0.00328							0.00698			4.7	15.1		
		-1.31	0.00957	0.00299							0.00636			4.5	13.7		
		-1.31	0.00831	0.00290							0.00616			4.5	12.4		
		-1.31	0.00905	0.00339	0.00924	0.00123	0.00313	0.00021	-6.32	-1.97	0.00722	0.00665	0.00044	4.8	12.6	13.1	1.3
Lepe Trench 4	4.1	-0.31	0.00864	0.00306							0.00651			4.6	12.5		
		-0.31	0.01438	0.00295							0.00628			4.5	19.3		
		-0.31	0.01208	0.00292							0.00622			4.5	16.7		
		-0.31	0.01455	0.00283							0.00602			4.4	19.9		
		-0.31	0.01203	0.00312	0.01234	0.00239	0.00298	0.00011	-7.79	-1.94	0.00663	0.00633	0.00024	4.6	16.3	17.0	2.9

Table 6. Isotope measurements from ostracods from Unit 2d.

Section / test pit / borehole	Field code	Laboratory code	Field moisture (%)	K conc. (%)	Th conc. (%)	U conc. (%)	Overburden thickness (m)	Cosmic dose rate (Gy/ka)	Total dose rate (Gy/ka)	Mean recycling ratio (all aq)	Mean D _e (Gy) (all accepted aq)	Age estimate (ka)	Age range (ka)	MIS attribution
Unit 5 (Brickearth)														
S1	LEP10-01	X4102	6.0	1.19±0.06	6.9±0.345	2.2±0.11	0.41	0.20±0.05	2.19±0.15	1.07	10.6±8.16	4.8 ± 3.7	1.1-8.5	1
S1	LEP10-02 (replicate of -01)	X4103	6.0	1.16±0.06	7.1±0.36	2.1±0.1	0.38	0.20±0.06	2.16±0.11	1.00	116.5±27.6	54 ± 13.1	41-67	4-3
S1	LEP10-03	X4104	14.0	1.24±0.06	11.4±0.57	2.6±0.13	0.79	0.19±0.03	2.36±0.16	1.08	5.2±3.06	2.2 ± 1.3	0.9-3.5	1
S1	LEP10-04 (replicate of -03)	X4105	14.0	1.24±0.06	11.4±0.57	2.6±0.13	0.76	0.19±0.03	2.24±0.11	1.01	73.7±35.2	32.9 ± 15.8	17-49	3-2
Unit 4 (Lepe Upper Gravel / St Leonards Farm Gravel [upper] – see Briant <i>et al.</i> , 2006a)														
S5	LEPE03-05	X1729	2.0	0.54±0.027	<0.300 (0.200±0.100)	1.25±0.063	2.00	0.16±0.04	0.68±0.06	1.04	38.9±2.7	57± 6	63-51	4–3
Unit 1 (Lepe Lower Gravel/St Leonards Farm Gravel [lower] – see Briant <i>et al.</i> , 2006a)														
S1	LEPE03-01	X1725	9.2	0.348±0.017	0.340±0.017	2.610±0.131	4.27	0.12 ±0.02	0.61 ±0.03	0.99	121.9 ± 6.3	198 ± 15	213-184	7–6
S1	LEPE03-02 (replicate of -01)	X1726	9.2	0.240±0.012	1.900±0.095	0.500±0.025	4.27	0.12 ±0.02	0.68 ±0.03	1.05	98.9 ± 3.4	146 ± 10	156-136	6
TP4a	LEPE03-03	X1727	17.9	0.138±0.007	0.420±0.021	1.16±0.058	5.00	0.11±0.01	0.36±0.02	1.02	50.7±2.30	141±11	152-130	6–5e
TP4a	LEPE03-04 (replicate of -03)	X1728	17.9	0.160±0.008	0.900±0.045	0.300±0.015	5.00	0.11±0.01	0.34±0.02	1.03	56.2±2.9	165±14	179-151	6

Table 7. OSL dosimetry, equivalent dose and age estimates for samples from the Stone Point SSSI sequence, Hampshire, England by PASHCC (Briant *et al.*, 2006a, 2009, Supplementary Information). Gy = Grays, ka = thousands of years. Dose rate estimate for Units 1 and 4 based on neutron activation analysis (NAA) and gamma spectrometry where feasible (LEPE03-01, 02, 05) and NAA alone where this was not possible (LEPE03-03, 04). Dose rate estimate for Unit 5 based on Inductively-Coupled Plasma Mass Spectrometry (ICP-MS). Age calculated by dividing mean D_e by total dose rate. Error quoted as one standard error (standard deviation / \sqrt{n}). MIS boundaries are taken from Shackleton *et al.* (1990) and Bassinot *et al.* (1994).

NEaar no.	Sample name	Asx D/L	Glx D/L	Ser D/L	Ala D/L	Val D/L	[Ser]/[Ala]
3312bF	LeBto1bF	0.680 ± 0.001	0.186 ± 0.001	0.987 ± 0.007	0.345 ± 0.001	0.214 ± 0.006	0.565 ± 0.002
3312bH*	LeBto1bH*	0.580 ± 0.000	0.180 ± 0.000	0.671 ± 0.013	0.267 ± 0.000	0.144 ± 0.002	0.489 ± 0.020
3313bF	LeBto2bF	0.680 ± 0.032	ND	0.749 ± 0.018	0.373 ± 0.003	ND	0.461 ± 0.005
3313bH*	LeBto2bH*	0.568 ± 0.003	0.168 ± 0.001	0.615 ± 0.122	0.268 ± 0.013	0.152 ± 0.005	0.316 ± 0.146

Table 8. Amino acid data on opercula of *Bithynia tentaculata* from Lepe. Error terms represent one standard deviation about the mean for the duplicate analyses for an individual sample. Each sample was bleached (b), with the free amino acid fraction signified by ‘F’ and the total hydrolysable fraction by ‘H*’. The sample size for 3313bF was very small, with concentrations similar to the level of detection, and therefore should be treated with caution.